Supplementary Materials for

Molecular Modification of $MAPbI_3$ Surface: Insights from First-Principles Theory Studies

Xin Ye, Wen Ou, Bin Ai, Yecheng Zhou**

School of Materials Science & Engineering, Sun Yat-sen University, Guangzhou 510006, Guangdong, People's Republic of China.

** Corresponding author. Email address: zhouych29@mail.sysu.edu.cn (Y. Zhou)*

Contents

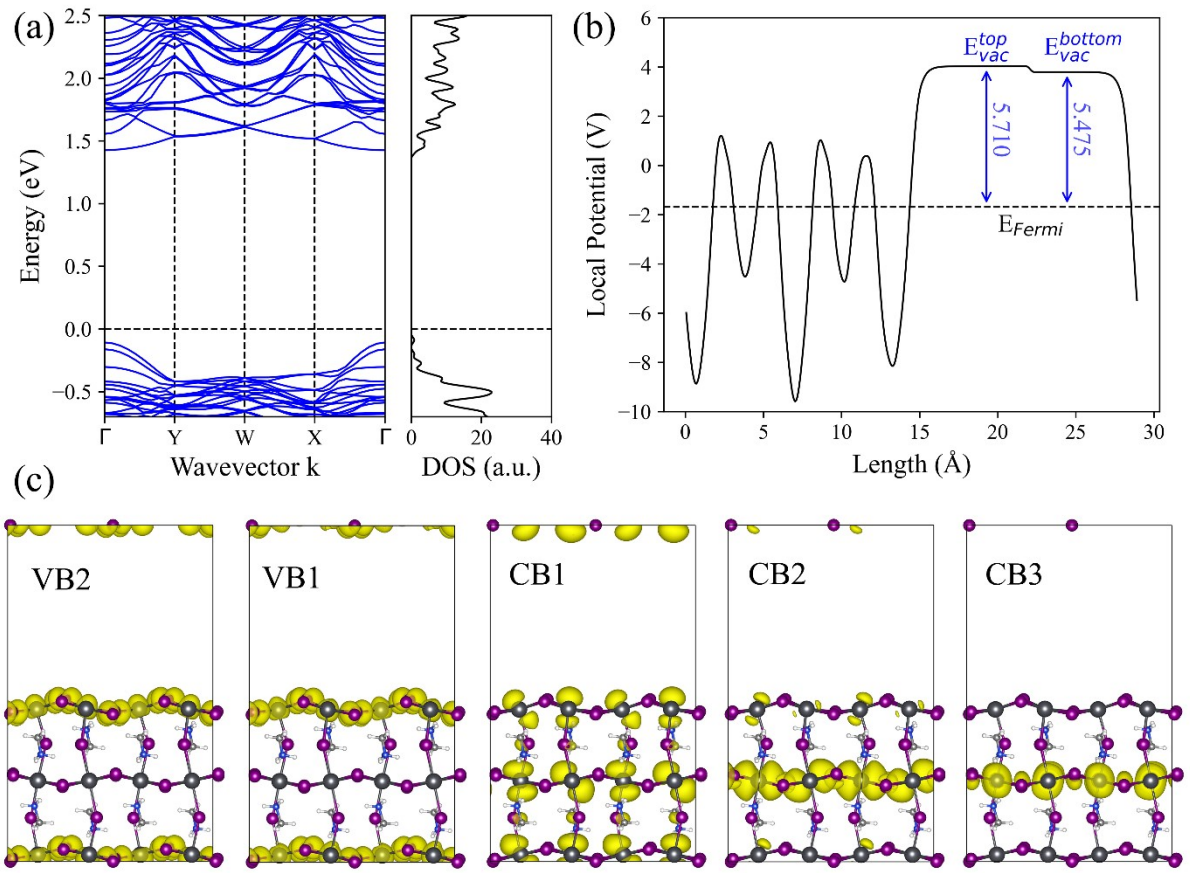

Fig. S1 (a) Band structure and DOS (Fermi energy level is set to zero); (b) Local potential curve along the z-axis; (c) VB2, VB1, CB1, CB2, and CB3 Γ point orbitals (isosurface level is set to 0.003 e/Bohr^3) of pristine $MAPbI_3$ surface.

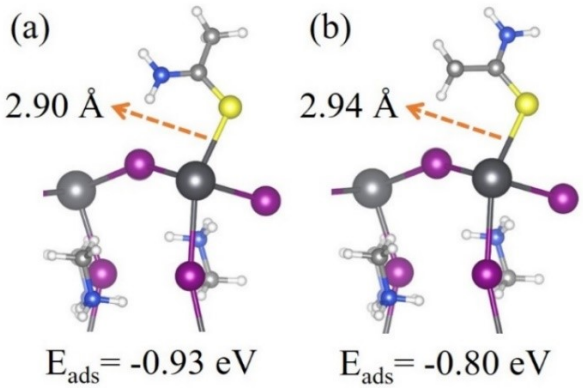

Fig. S2 Side views of the (a) minimum energy configuration and (b) C-N exchanged configuration of CC(=S)N adsorption.

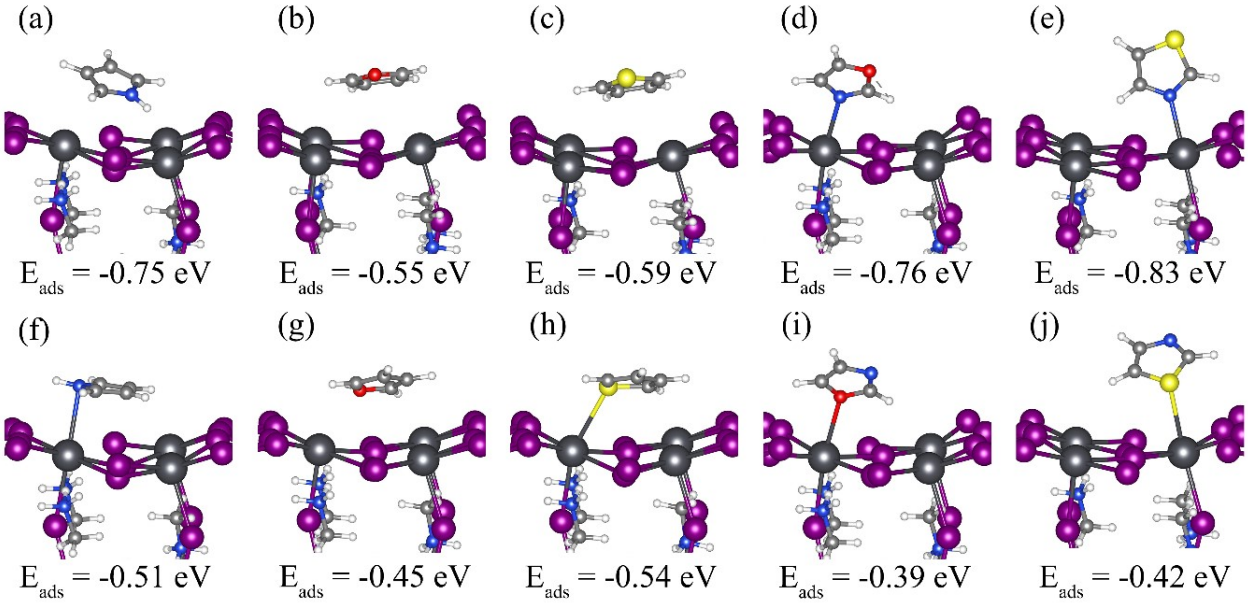

Fig. S3 The minimum energy configurations and adsorption energies of (a) R5-N@PVK, (b) R5-O@PVK, (c) R5-S@PVK, (d) R5-O-3N@PVK, and (e) R5-S-3N@PVK. The configurations that Pb sites linked by linking atoms and adsorption energies of (f) R5-N@PVK, (g) R5-O@PVK, and (h) R5-S@PVK. The configurations that the positions of O (S) and N are exchanged and adsorption energies of (i) R5-O-3N@PVK, and (j) R5-S-3N@PVK.

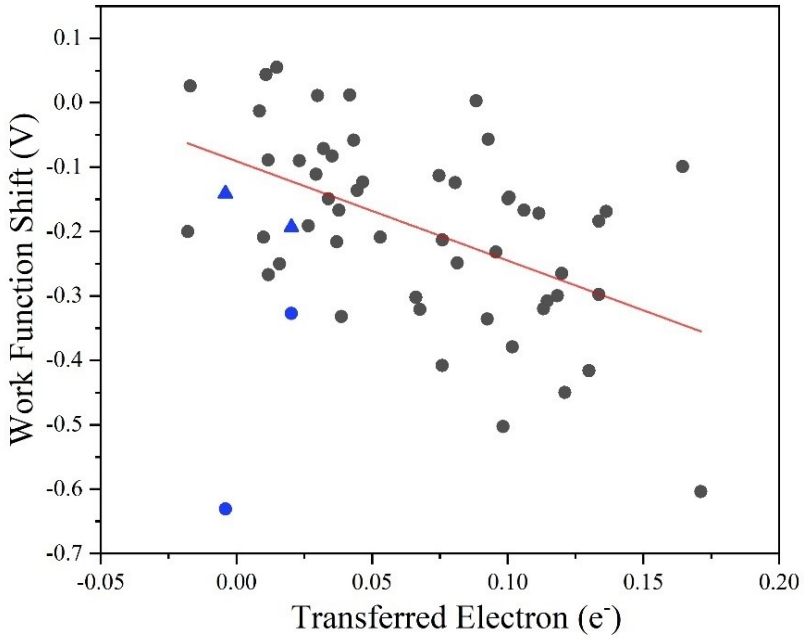

Fig. S4 Transferred charges against WFS, and their linear fitting. The WFS of blue points (R6-1,4O and R6-O-4H adsorptions with midgap defect) are corrected so that they are moved into triangle points.

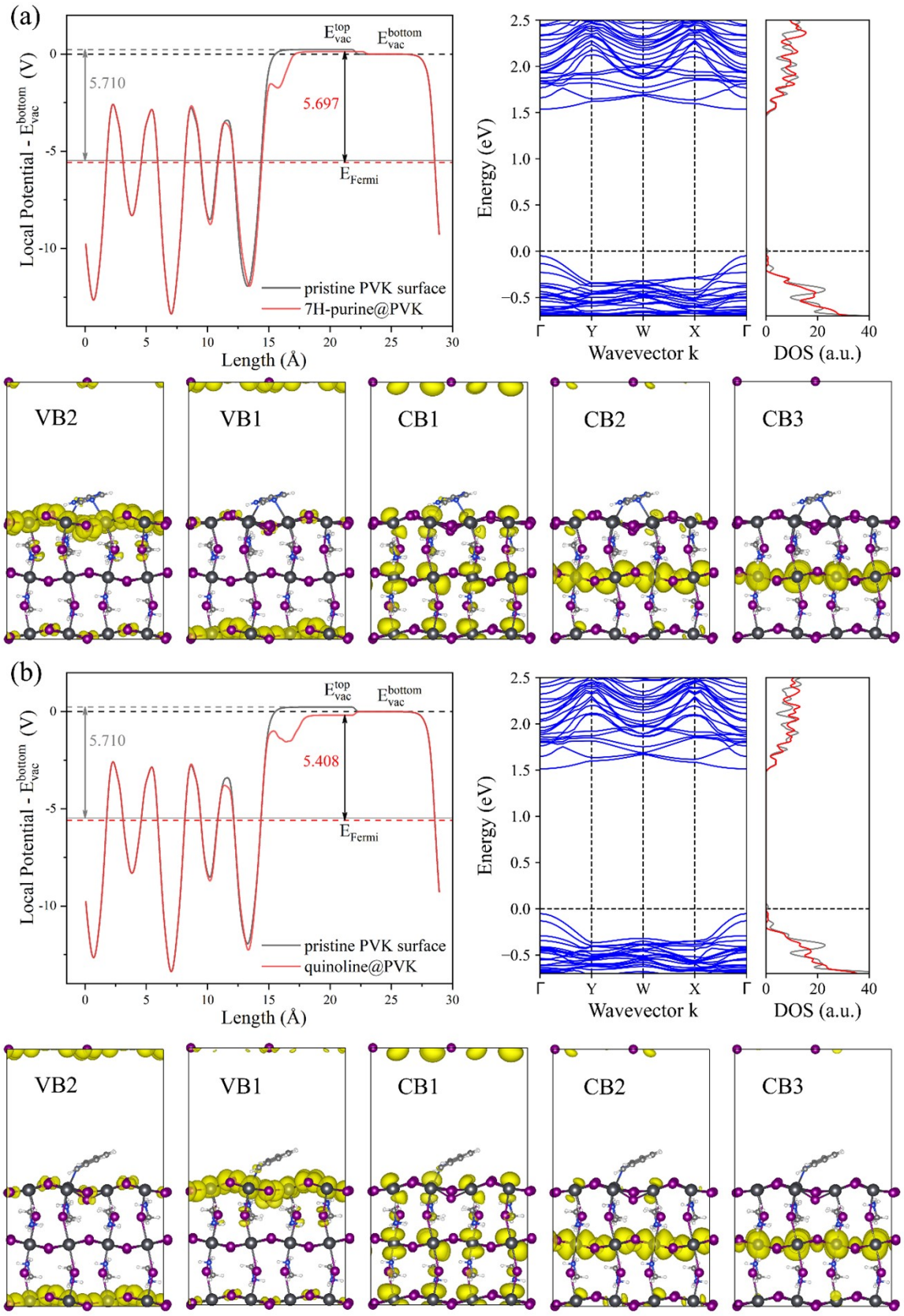

Fig. S5 The local potential curves, band structures, DOS, and orbitals of (a) 7H-purine@PVK and (b) quinoline@PVK. The grey line in DOS represents the DOS of the pristine PVK surface that is aligned for comparison.

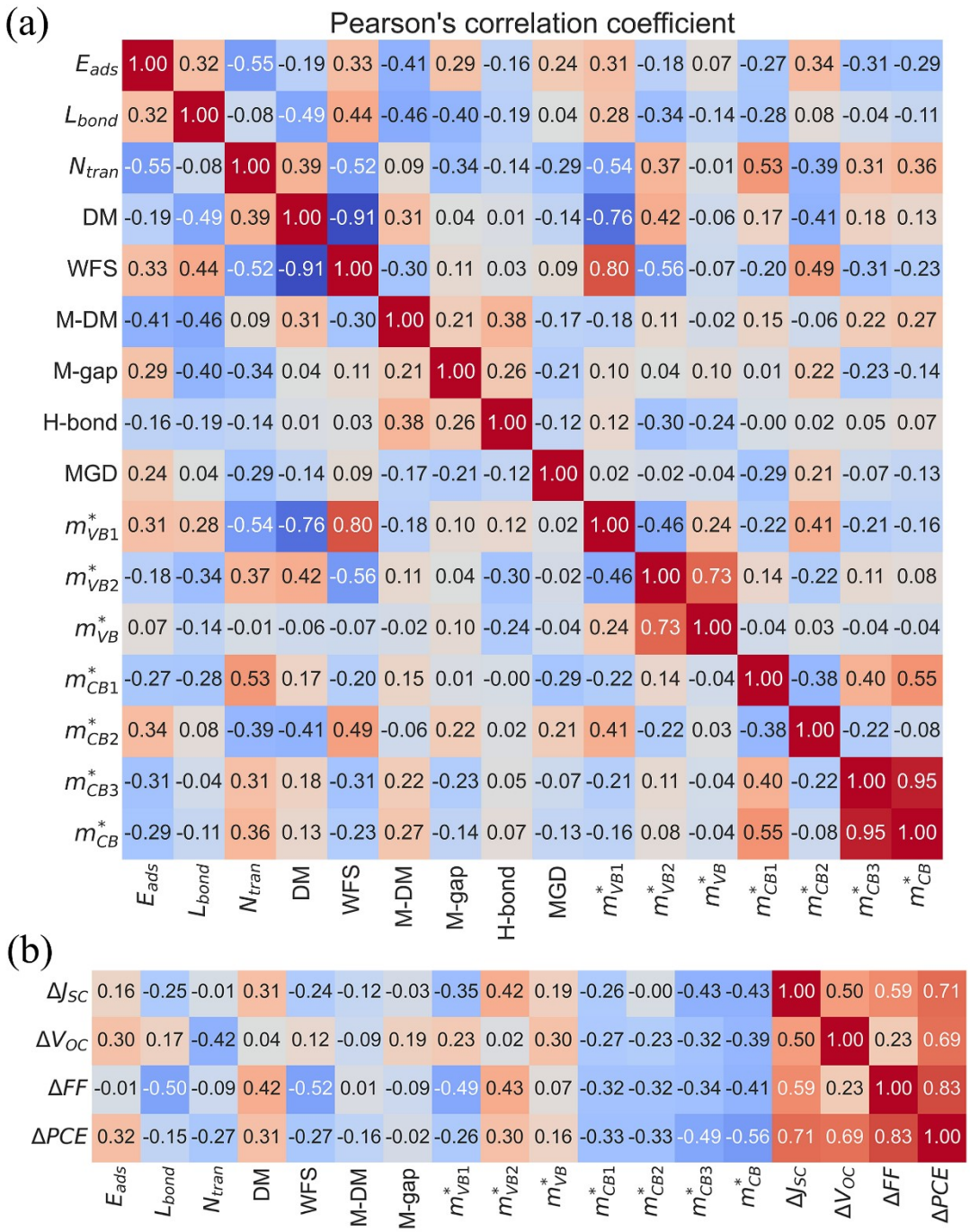

Fig. S6 Pearson's correlation coefficient of (a) the calculated physical quantities in Table 1, Table 2, and Table S1, and (b) the PV performance and calculated physical quantities from the modifiers listed in Table S2. 1/0 is used to represent whether the H-bond or MGD exists or not. All the data has been normalized. Note that E_{ads}, m^*_{VB1}, m^*_{VB2}, and m^*_{VB} are negative.

Table S1 Data for molecule adsorptions. L_{bond} represents bond length in *Linkage*. When the *Linkage* is "co-plane", the *Length* represents the average distance between the molecule and the surface. *Angle* represents the angle between the molecular plane and the (001) surface for ring-based molecules or the angle between the bond and the (001) surface for linear molecules. *H··I* and *π··Pb* represent that if there are hydrogen bonds with I ion and conjunction interaction with Pb ion obviously observed from charge density difference, respectively, where Y means "yes", and N means "no". The number in [ ] means the corrected value of WFS. M-DM and M-gap represent the molecular net dipole moment and the molecular band gap, respectively.

Class	Notion of molecule	Linkage	L_{bond} (Å)	Angle (°)	E_{ads} (eV)	N_{tran} (e^-)	DM (a.u.)	WFS (eV)	H··I	π··Pb	M-DM (D)	M-gap (eV)
Linear	CO	Pb-O-C	2.629	~60	-0.620	0.038	0.222	-0.167	Y	N	1.657	12.865
	COC	Pb-O(-C)(-C)	2.662	~60	-0.647	0.027	0.382	-0.191	N		1.246	12.574
	CS	Pb-S-C	3.036	30~60	-0.655	0.112	0.234	-0.172	N		1.590	11.040
	CSC	Pb-S(-C)(-C)	3.061	~60	-0.740	0.113	0.390	-0.320	N		1.608	10.963
	CN	Pb-N-C	2.577	~30	-1.057	0.134	0.491	-0.298	N		1.328	11.754
	CN(C)C	Pb-N(-C)(-C)(-C)	2.691	0~30	-0.930	0.120	0.207	-0.265	N		0.545	10.989
	CN=NC	Pb-N(=N)(-C)	2.832	60~90	-0.720	0.101	0.000	-0.147	N		0.001	9.599
	CC≡N	Pb-N≡C	2.683	0~30	-0.574	0.034	0.397	-0.149	N		4.039	14.128
	CC(=O)C	Pb-O=C	2.580	30~60	-0.688	0.039	0.646	-0.332	N		3.030	10.709
	CC(=O)N	Pb-O=C	2.445	~30	-0.986	0.068	0.519	-0.321	Y		3.911	11.900
	NC(=O)N	Pb-O=C	2.443	~0	-1.099	0.037	0.251	-0.216	Y		3.864	11.988
	CC(=S)C	Pb-S=C	3.046	0~30	-0.670	0.115	0.367	-0.308	N		2.933	8.065
	CC(=S)N	Pb-S=C	2.903	30~60	-0.930	0.171	1.052	-0.604	Y		4.619	8.829
	NC(=S)N	Pb-S=C	2.847	0~30	-1.247	0.165	-0.188	-0.099	Y		5.232	9.557
	CC(=O)O	Pb-O=C	2.538	~60	-0.647	0.010	0.422	-0.209	Y		1.779	12.209
	CC(=O)OC	Pb-O=C	2.521	0~30	-0.764	0.012	0.583	-0.267	N		4.555	12.040

	CC(=O)SC	Pb-O=C	2.513	0~30	-0.816	0.016	0.471	-0.250	N		4.270	10.512
	CS(=O)(=O)C	Pb-O=S	2.574	30~60	-0.820	0.011	-0.524	0.044	N		4.525	12.983
	CS(=O)(=O)N	Pb-O=S	2.613	~30	-0.756	-0.018	0.454	-0.200	Y		3.548	13.178
Five-member Ring (R5)	R5-O	co-plane	3.160	0~30	-0.550	0.043	-0.049	-0.058	N	Y	0.578	10.613
	R5-S	co-plane	3.223	0~30	-0.594	0.042	-0.051	0.012	N	Y	0.508	10.089
	R5-N	co-plane	3.038	~30	-0.746	0.088	-0.358	0.003	N	Y	1.935	10.776
	R5-2N	Pb-N(=C)(-C)	2.528	60~90	-0.990	0.130	0.802	-0.416	N	N	2.148	10.077
	R5-3N	Pb-N(=C)(-C)	2.588	30~60	-0.972	0.096	0.509	-0.232	N	N	2.541	9.775
	R5-1,2N	Pb-N(-N)(=C)	2.584	30~60	-1.005	0.075	0.198	-0.113	Y	N	2.320	11.345
	R5-1,3N	Pb-N(=C)(-C)	2.568	~60	-1.011	0.121	0.972	-0.450	N	N	3.802	11.036
	R5-1,2,4N	Pb-N(-N)(=C)	2.740	0~30	-0.895	0.030	-0.155	0.011	Y	N	2.913	11.681
	R5-O-3N	Pb-N(=C)(-C)	2.633	30~60	-0.760	0.081	0.427	-0.249	N	N	1.594	10.931
	R5-S-3N	Pb-N(=C)(-C)	2.578	60~90	-0.828	0.102	0.564	-0.379	N	N	1.635	10.137
Six-member Ring (R6)	R6-N	Pb-N(=C)(-C)	2.694	~30	-0.936	0.076	0.372	-0.213	N	N	2.247	10.275
	R6-1,2N	Pb-N(-N)(=C)	2.655	30~60	-0.975	0.075	0.804	-0.408	N	N	4.231	9.048
	R6-1,3N	Pb-N(=C)(-C)	2.634	~90	-0.857	0.121	0.615	-0.336	N	N	2.347	9.856
	R6-1,4N	Pb-N(=C)(-C); Pb-N(=C)(-C)	2.913; 2.941	~0	-0.869	0.032	0.000	-0.071	N	N	0.000	9.459
	R6-1,2,4N	Pb-N(=C)(-C); Pb-N(=N)(-C)	2.888; 3.138	~0	-0.764	0.012	0.000	-0.089	N	N	2.650	8.633
	R6-1,3,5N	Pb-N(=C)(-C)	2.722	30~60	-0.696	0.047	0.000	-0.123	N	N	0.001	10.205
	R6-O-4H	Pb-O(-C)(-C)	2.803	30~60	-0.521	0.020	0.177	-0.327 [-0.193]	N	N	0.874	9.871

	R6-1,4O	Pb-O(-C)(-C)	2.937	~0	-0.697	-0.004	0.000	-0.631 [-0.141]	N	N	0.001	9.070
Phenyl Group (Ph)	Ph	co-plane	3.316	~0	-0.576	0.029	0.000	-0.111	N	Y	0.000	10.632
	Ph-F	co-plane	3.631	0~30	-0.503	0.015	-0.214	0.055	N	Y	1.474	10.218
	Ph-C	co-plane	3.412	0~30	-0.690	0.035	0.019	-0.083	N	Y	0.392	10.298
	Ph-O	co-plane	3.341	0~30	-0.573	-0.017	0.061	0.026	Y	N	1.301	9.775
	Ph-S	Pb-S-C	3.190	~0	-0.959	0.100	-0.053	-0.149	N	Y	1.140	9.438
	Ph-N	Pb-N-C	2.691	0~30	-0.992	0.106	0.252	-0.167	N	N	1.603	9.359
	Ph-N-4F	Pb-N-C	2.672	0~30	-1.003	0.081	0.123	-0.124	N	N	2.884	9.042
	Ph-N-2,4,6F	Pb-N-C	2.748	0~30	-0.848	0.053	0.228	-0.209	N	N	1.692	9.388
	Ph-N-2,3,4,5,6F	Pb-N-C	2.807	0~30	-0.800	0.023	0.028	-0.090	N	N	3.047	9.763
Combination	naphthalene	co-plane	3.327	~0	-0.876	0.045	0.000	-0.136	N	Y	0.000	8.500
	1H-indole	co-plane	3.169	~0	-0.966	0.093	-0.132	-0.057	N	Y	2.157	9.023
	quinoline	Pb-N(=C)(-C)	2.785	30~60	-0.999	0.066	0.267	-0.302	N	N	2.077	8.622
	7H-purine	Pb-N(=C)(-C); Pb-N(=C)(-C)	2.868; 2.943	0~30	-1.176	0.009	-0.361	-0.013	Y	N	3.682	9.517
	3-phenylpyrrole	co-plane	3.406	0~30	-1.155	0.118	0.282	-0.300	N	Y	2.427	9.032
	4-phenylpyridine	Pb-N(=C)(-C)	2.647	30~60	-1.131	0.098	0.751	-0.503	N	N	2.732	9.190
	2-thiophenamine	Pb-N-C	2.830	~0	-1.027	0.134	0.389	-0.184	N	Y	1.651	9.314
	3-thiophenamine	Pb-N-C; Pb-S(-C)(-C)	2.711; 3.363	~0	-1.067	0.136	0.357	-0.169	N	N	1.811	9.214

Table S2 PV performance for the molecules applied in experiments. The "-pre" represent the parameters for untreated PSCs. The "-post" represent the parameters for treated PSCs.

Notion of molecule	ΔJ_{SC} (mA/cm^2)	ΔV_{OC} (V)	ΔFF (%)	ΔPCE (%)	PVK type	Position	Ref
NC(=S)N	23.36→23.53	1.070→1.080	77.0→77.0	19.25→19.57	FAMAPbI	precursor	3
NC(=O)N	20.91→21.26	1.049→1.089	72.0→75.0	16.80→18.25	MAPbI	precursor	2
R5-1,3N	22.18→22.88	1.060→1.110	77.5→79.3	18.22→20.13	MAPbI	PVK/HTL	6
Ph-N-4F	20.47→22.16	1.000→1.070	66.6→73.2	13.63→17.35	MAPbI	PVK/HTL	10
quinoline	22.48→23.07	1.108→1.142	74.9→79.2	18.65→20.87	FAMACsPbIBr	precursor	11
Ph-N	22.30→23.00	0.960→0.930	65.0→64.0	14.20→13.80	FAPbI	precursor	9
R6-N	20.70→24.10	0.950→1.050	68.0→72.0	13.10→16.50	MAPbI	PVK/HTL	4
R6-1,4N	22.43→22.83	1.092→1.133	78.2→79.5	19.14→20.58	FAMAPbI	precursor	8
R5-S-3N	19.04→21.04	1.033→1.044	73.0→82.0	14.34→17.89	MAPbI	PVK/HTL	7
R5-N	22.26→22.99	1.101→1.142	75.8→76.3	18.58→20.07	FAMACsPbI	precursor	5
R5-S	20.70→21.30	0.950→1.020	68.0→68.0	13.10→15.30	MAPbI	PVK/HTL	4

Definition and Calculation of the Mentioned Physical Quantities

The adsorption energy is defined by:

$$E_{ads} = E_{final} - E_{initial} = E_{pm} - E_m - E_p \quad (1)$$

where E_{pm}, E_p, and E_m represent the total energies of the molecule-adsorbing PVK surface, the pristine PVK surface, and the molecule, respectively.

The effective masses of charge carries are calculated by:

$$\frac{1}{m^*} = \frac{1}{\hbar} \frac{d^2E(k)}{dk^2} \quad (2)$$

m^* is the effective mass. $\hbar$ is the reduced Planck constant. $E(k)$ is the energy of a band and k is the wave vector. The second derivatives are calculated as the quadratic coefficient (a) obtained by polynomial fitting:

$$E(k) = a(k - k_0)^2 + c \quad (3)$$

The k_0 is the wave vector whose energy is the minimum (maximum) of the conduction (valence) band. Fifty points are inserted between Γ and Y (or Γ and X), in which 8 points near Γ points are chosen to fit the parabolic function.

The work function shift (WFS) is defined by the difference between the WF of the molecule-adsorbing PVK surface (WF_{pm}) and the pristine PVK surface ($WF_p = 5.71\ eV$):

$$WFS = WF_{pm} - WF_p = (E_{pm}^{vac\_top} - E_{pm}^{Fermi}) - (E_p^{vac\_top} - E_p^{Fermi}) \quad (4)$$

The $E_{pm}^{vac\_top}$ and $E_p^{vac\_top}$ represent the top surface vacuum energy levels of the two, respectively. The E_{pm}^{Fermi} and E_p^{Fermi} represent the Fermi energy levels of the two, respectively.

Choice and Generalization of PVK Surface

According to previous work[1, 2], (110)-flat, (110)-vacant, (001)-flat, and (001)-vacant surface are the four possible surfaces of β-phase $MAPbI_3$, as shown in Fig. S7. Firstly, their surface energies were calculated.[2-4] Assuming that the system is under equilibrium for Pb, I_2, MAI, PbI_2, and $MAPbI_3$ phases, the thermodynamic stable range of μ_{Pb} and μ_I for $MAPbI_3$ is represented as:

$$\Delta H(MAPbI_3) - \Delta H(MAI) \leq \mu_{Pb} + 2\mu_I \leq \Delta H(PbI_2) \tag{5}$$

Referred to our calculation, $\Delta H(MAPbI_3) - \Delta H(MAI) = -2.181\ eV$, $\Delta H(PbI_2) = -2.180\ eV$. The phase diagram is shown in Fig. S7e. Under the condition of $\mu_{Pb} + 2\mu_I = -2.180\ eV$, the surface energies of the (110)-flat, (110)-vacant, (001)-flat, and (001)-vacant surface are 1.31 eV/nm^2, 1.33 eV/nm^2, 1.49 eV/nm^2, and 1.45 eV/nm^2, respectively. The (110) surfaces have lower surface energies than the (001) surface, which agrees with the work of Tateyama et al.[2] Additionally, as the formation energies of vacant and flat terminations are too closed, they should coexist in experiments. The band gap of the (110)-flat, (110)-vacant, (001)-flat, and (001)-vacant surfaces are 1.38 eV, 1.71 eV, 1.31 eV, and 1.62 eV, respectively. Flat termination has a narrower band gap that mainly decides the charge transport.[2]

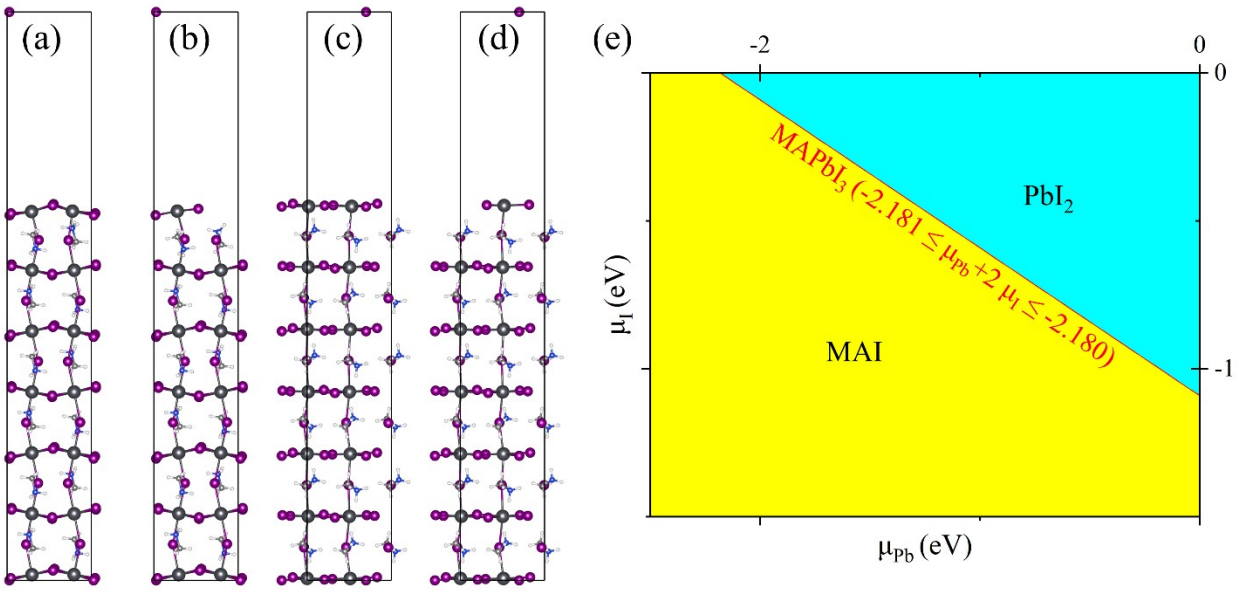

Fig. S7 Optimized (a) (110)-flat, (b) (110)-vacant, (c) (001)-flat, and (d) (001)-vacant surface of β-phase $MAPbI_3$. (e) Calculated phase diagram of $MAPbI_3$.

To justify the generalization of our calculation, we selected four representative molecules, $R6\_1,2,4N$, $R6\_1,4O$, 7H-purine, and quinoline, to modify the four surfaces mentioned ($2\sqrt{2} \times 2\sqrt{2}$) and one $FAPbI_3$ surface (2×2), which produced twenty models. Table S3 shows their adsorption energies. The (110) surface produces stronger adsorption energies than the (001) surface probably due to its rugged morphology. Although the values of adsorption energies of these molecules differ, the trend of these adsorption energies is almost the same.

Table S3 Adsorption energies (eV) of R6-1,2,4N, R6-1,4O, 7H-purine, and quinoline modifications on (110)-flat, (110)-vacant, (001)-flat, (001)-vacant β-phase $MAPbI_3$ surfaces, and (001)-flat α-phase $FAPbI_3$ surface.

Surface	R6-1,2,4N	R6-1,4O	7H-purine	quinoline
(110)-flat β-$MAPbI_3$	-0.76	-0.70	-1.18	-1.00
(110)-vacant β-$MAPbI_3$	-0.61	-0.41	-0.76	-0.74
(001)-flat β-$MAPbI_3$	-0.11	-0.06	-0.47	-0.32
(001)-vacant β-$MAPbI_3$	-0.36	-0.01	-0.34	-0.53
(001)-flat α-$FAPbI_3$	-0.50	-0.48	-0.68	-0.63

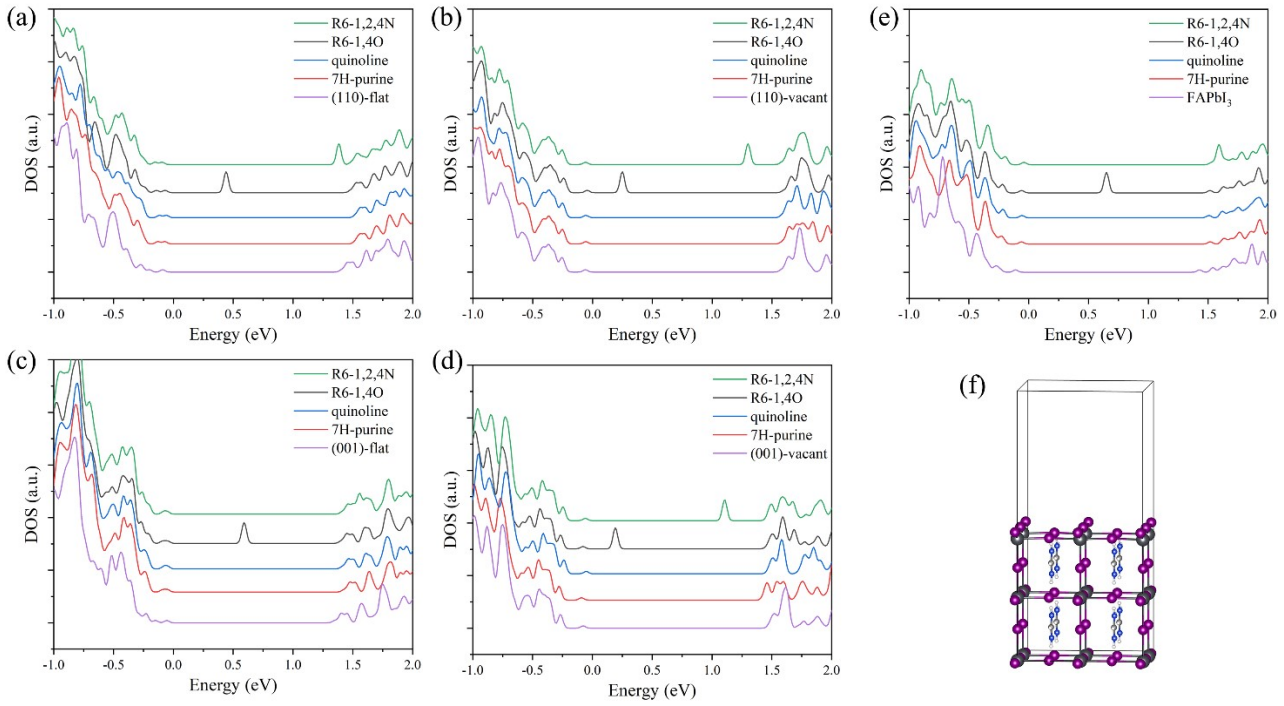

Fig. S8 DOS of R6-1,2,4N, R6-1,4O, 7H-purine, and quinoline modifications on (a) (110)-flat, (b) (110)-vacant, (c) (001)-flat, and (d) (001)-vacant surfaces of β-phase $MAPbI_3$ and their pristine surfaces. (e) DOS of the modified and pristine surface of (001)-flat α-phase $FAPbI_3$. (f) Optimized pristine surface of flat α-phase $FAPbI_3$.

The electronic properties of these molecules on the four surfaces were also compared. Fig. S8 shows the DOS of the pristine five surfaces and twenty modified surfaces. The defect energy level of R6-1,4O is kept for all five surfaces. However, the defect energy level of R6-1,2,4N disappears in (001)-flat $MAPbI_3$ surface. 7H-purine influences the CB of vacant surfaces more than flat surfaces. Quinoline has little impact on each surface. Broadly, the changes induced by the four modifications induce have a degree of similarity. Even on $FAPbI_3$ surface, the impact of modification in electronic states is similar.

Considering that the (110)-flat β-$MAPbI_3$ surface has the lowest surface energy and low band gap, and the trend of molecule adsorption energy on various surfaces are similar as well as the electronic states, we take the (110)-flat β-$MAPbI_3$ surface as the representative surface for further investigation.

Adsorption Configuration Determination

The initial adsorption configuration is constructed with the following rules:

1. The non-carbon and non-hydrogen atom (such as S, O, N) is placed near the surface Pb atom, but slightly far away from the surface to avoid the formation of chemical bonds.
2. For molecules composed of only C and H, the π-conjugation plane is located above the Pb atom.
3. Molecules start in a lying down position along the surface

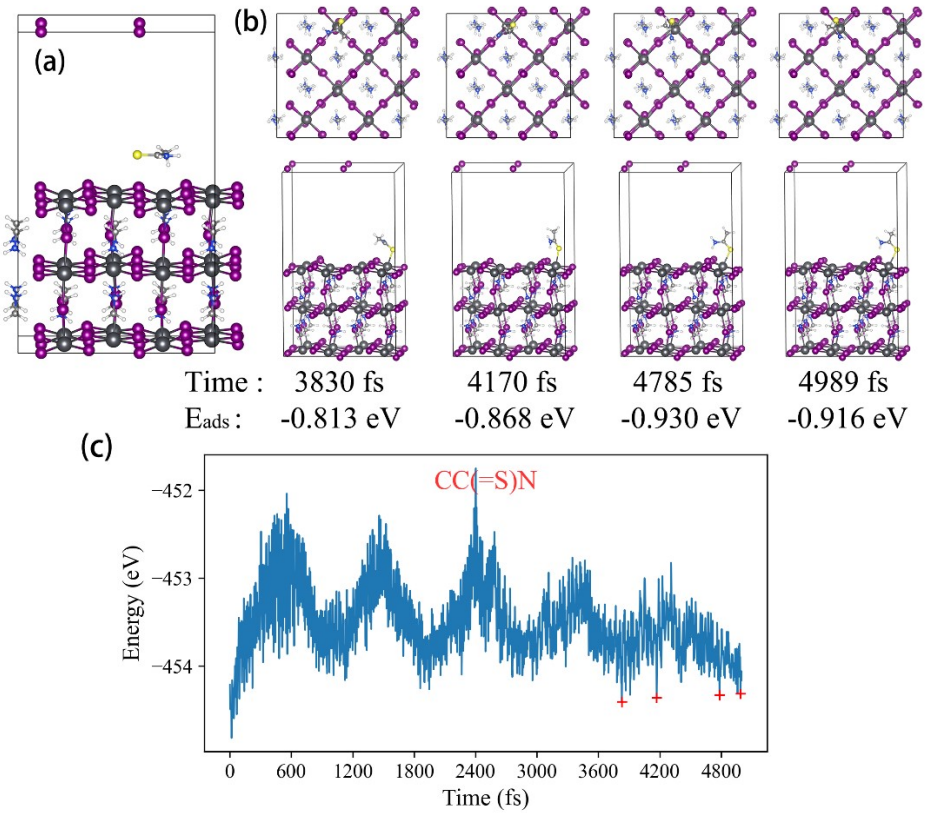

Fig. S9 (a) The initial adsorption configuration of CC(=S)N. (b) The optimized geometries at the four energy troughs and the adsorption energies. (c) Energy changes during the 5 ps AIMD. The red crosses mark the minimum energy points.

For example, Fig. S9a shows the initial adsorption configuration of the CC(=S)N on the PVK surface. N atom and S atom are located near the Pb atom, and the molecule is in a lying down position. After this 5 ps AIMD, 4 configurations located at energy troughs were chosen, as shown in Fig. S9b,c, for future geometry optimization. After optimization, the configuration with the lowest energy is reckoned as the most possible configuration. However, we also found that these four configurations obtained from AIMD may be unreasonable (not absorbed), some configurations were manually created and then optimized. Finally, the configuration with the minimum energy among all these configurations was chosen for future investigations.

To check the convergence of AIMDs, total energy change and molecular root mean square deviation (RMSD) of five modified surfaces as examples are shown in Fig. S11. Most of the molecules show relatively stable or limited changed RMSD after 4 ps. And their energies tend to fluctuate around a certain value after 1.5 ps. Their adsorption energies at the four troughs after geometry optimization and self-consistent calculation are listed in Table S4. Their adsorption energies do not change much at each trough. The configurations of every minimum energy configuration are shown in the last chapter of this document.

Table S4 Adsorption energies of CC(=S)N, R6-N, Ph-O, 7H-purine, and 2-thiophenamine at the four troughs after geometry optimization and self-consistent calculation. All unit are eV.

Trough	CC(=S)N	R6-N	7H-purine	2-thiophenamine
1	-0.81	-0.86	-1.18	-0.87
2	-0.87	-0.87	-1.01	-0.91
3	-0.93	-0.92	-1.03	-1.03
4	-0.92	-0.94	-0.93	-1.03

Molecules such as 2-thiophenamine could have a greater fluctuation in RMSD because its FG does not strongly interact with the surface. To illustrate this, we continue to perform another 20 ps AIMD for 2-thiophenamine, shown in Fig. S10. The amino group connected with the Pb ion during the AIMD, and the thiophene group persistently moved and rotated. However, as Table S4 and Fig. S10 show, the adsorption energies at the energy trough are similar (E_{ads} = -1.01 eV at 13,305 fs), indicating that a 5 ps AIMD could find a reasonable and stable adsorption configuration.

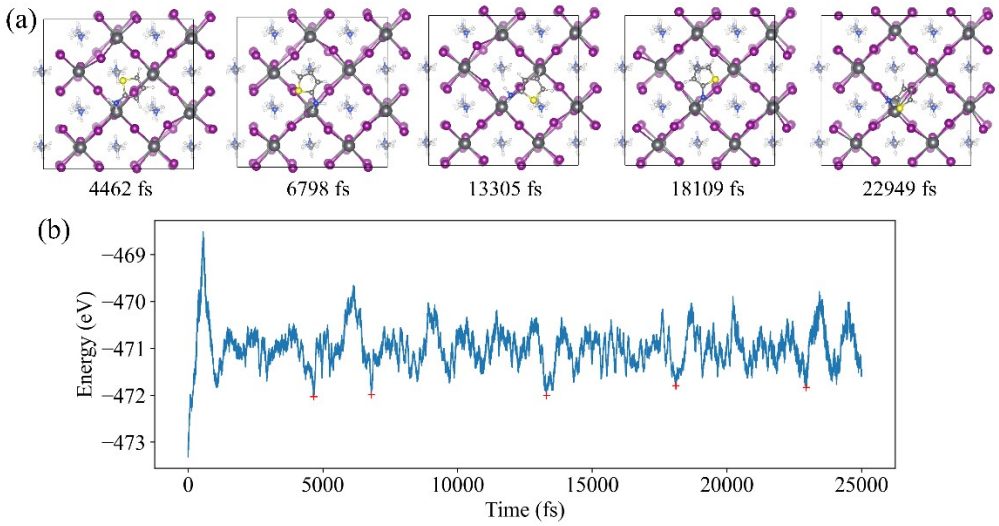

Fig. S10 (a) Minimum energy configurations of 2-thiophenamine during the 25 ps AIMD. (b) Total electronic energy changes during the 25 ps AIMD and the red crosses mark the minimum energy points.

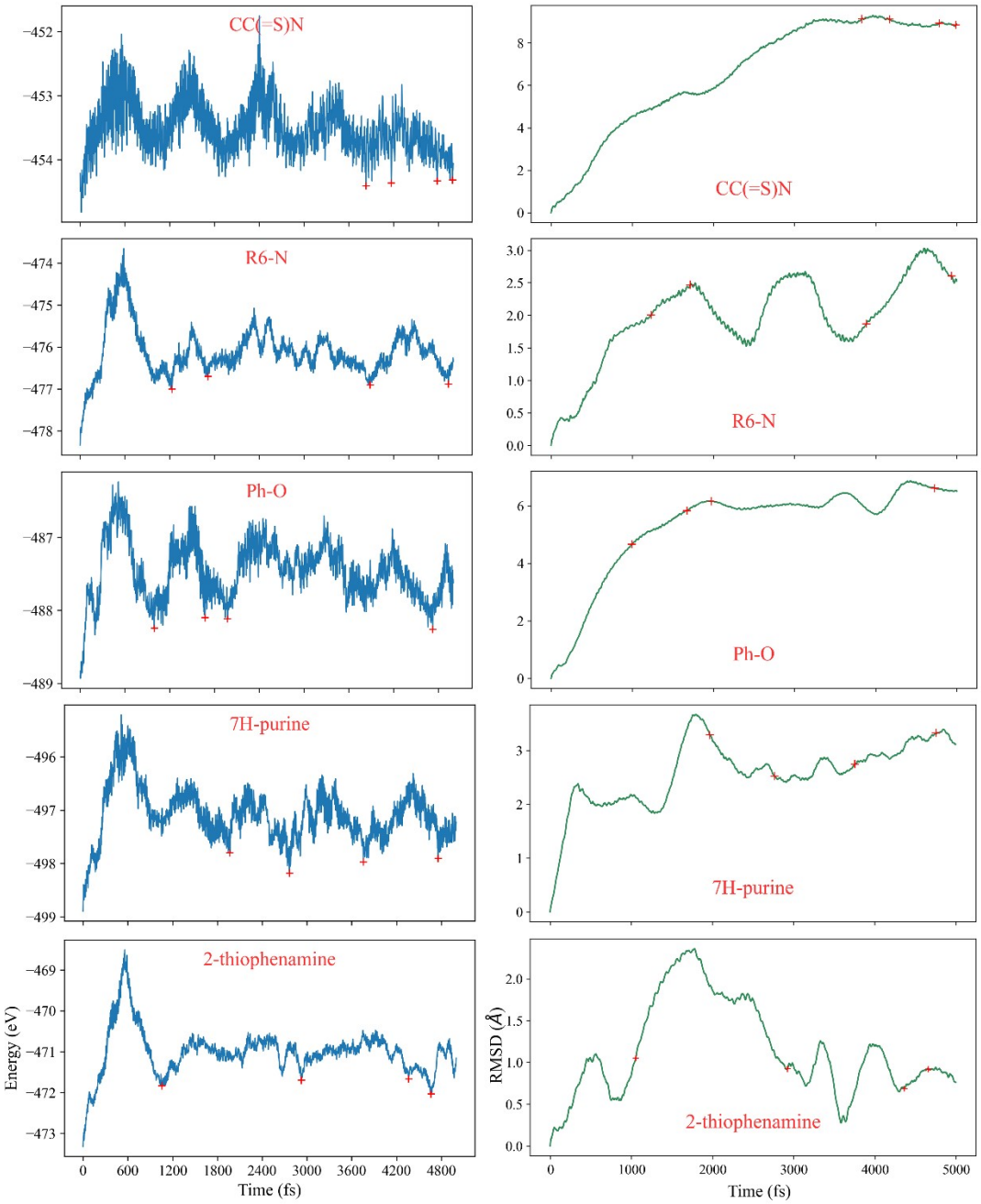

Fig. S11 The energy change and molecular RMSD of CC(=S)N, R6-N, Ph-O, 7H-purine, and 2-thiophenamine during AIMD. The four red crosses in each graph mark the chosen minimum energy points.

VB Orbitals Distribution

If the model has a relatively high WF on the top surface, the VB with orbital mainly distributing on the top surface tends to move downward, and vice versa. Therefore, the modified surface with increased or nearly unchanged WF tends to transport holes with the bottom surface and gives a smaller effective hole mass at VB1. For example, 7H-purine@PVK has a higher WF than quinoline@PVK and therefore its VB1 and VB2 orbitals are exchanged (Fig. S5). Fig. S12 exhibits that the WFS is broadly positively correlated with the effective mass of VB1, proving that the WFS directly influences the proportion of the orbital distribution.

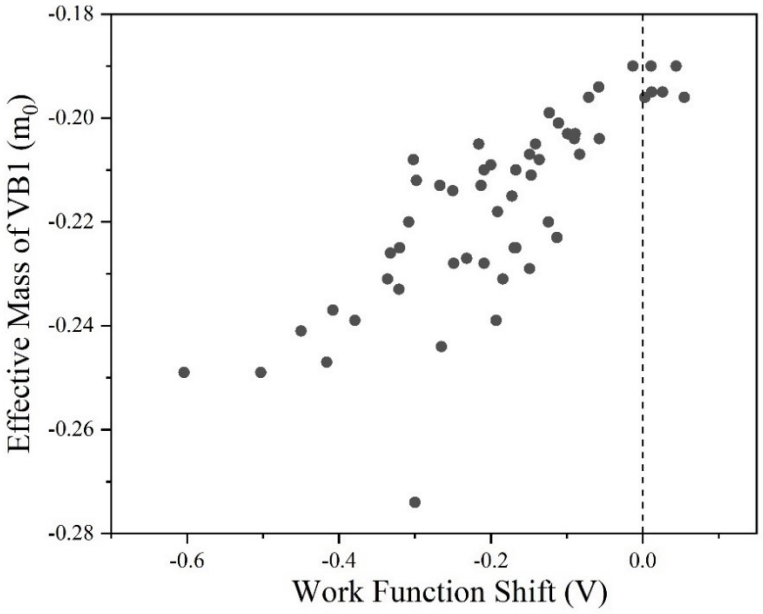

Fig. S12 WFS against effective mass of VB1. The WFS of R6-1,4O@PVK and R6-O-4H@PVK have been moved by replacing E_{Fermi}^{0} with $E_{Fermi}^{corrected}$. The nethermost point represents 3-phenylpyrrole@PVK.

Effective Mass versus Transport Property

The mobility of carriers can be obtained by:

$$\mu = \frac{q\tau}{m^*}$$

where q is the charge of the carrier (including charge), m^* is the effective mass of the charge carrier, τ is the carrier lifetime. Therefore, the effective mass is inversely proportional to mobility. Solar cell's performance with mobilities could be predicted by our previous work seen in the Fig. S13[16]. Therefore, the proportion of the effective mass change could impact PCE.

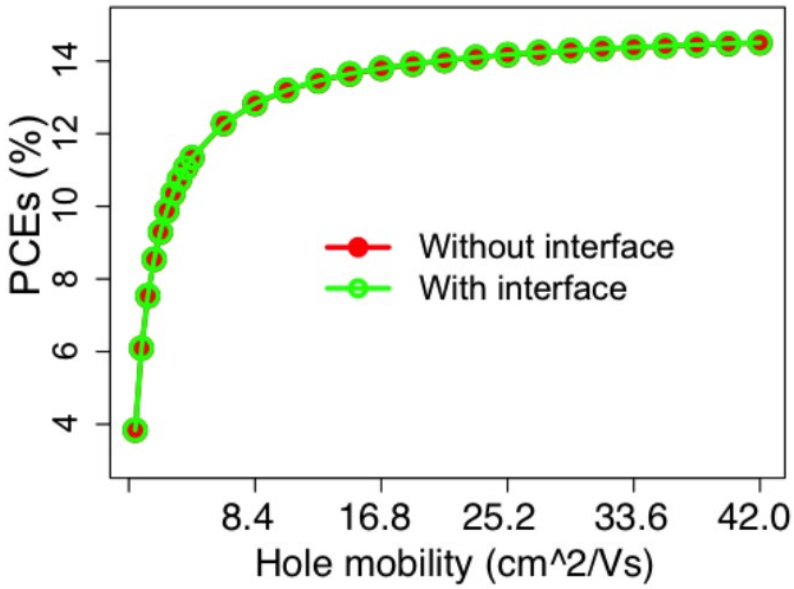

Fig. S13 Solar cell's performance with mobilities. Both the electron and hole mobilities increase at the same to certain times of 0.65 (electron) and 0.42 (hole) cm^2/Vs.

Modifier Design for Xanthine, Uric Acid, and Their Derivatives

Based on the experimental results of caffeine, theobromine, and theophylline by Wang et al. [17], we partly explained their experimental result in our insight and went a step further to add and replace groups to set an example for modifier design.

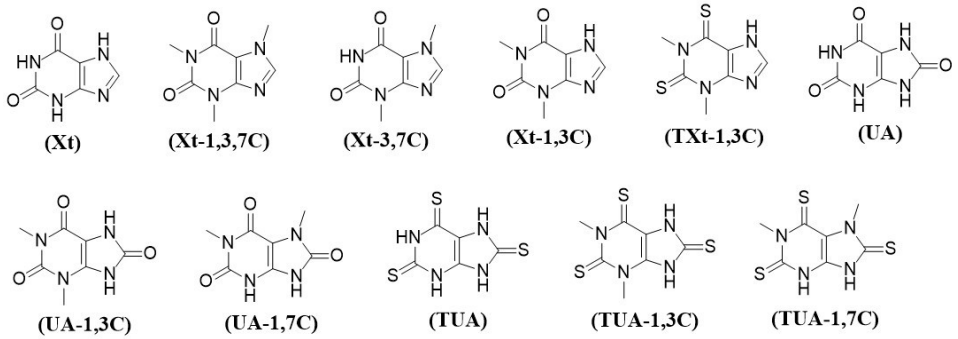

Fig. S14 Xanthine, uric acid, and their derivatives. The molecular notions with T are of sulfur substitution.

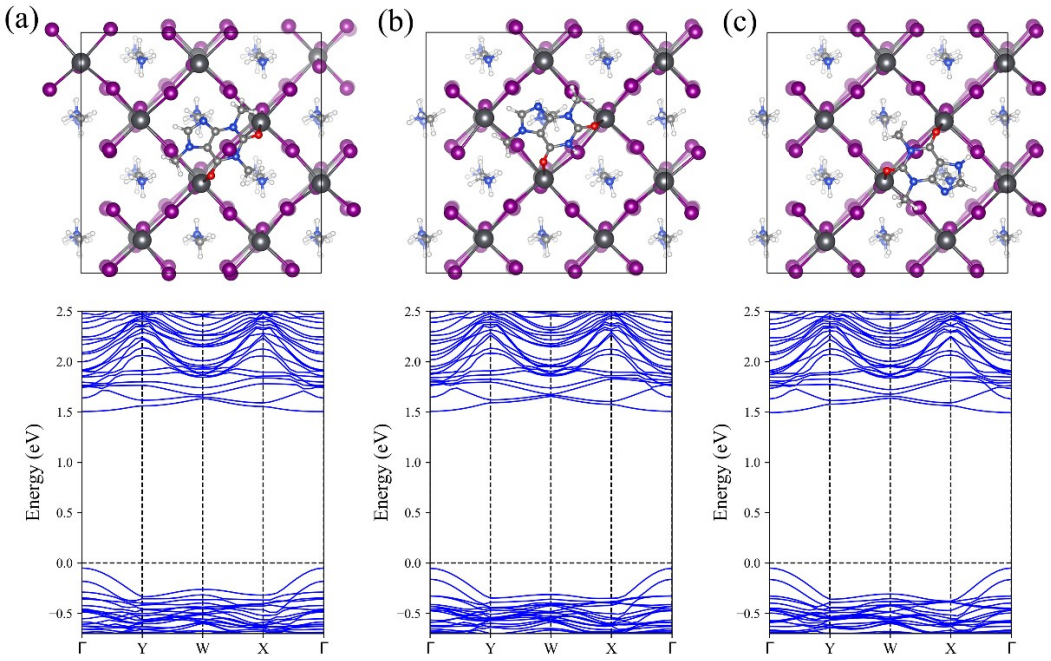

Fig. S15 Configurations and band structures of (a) Xt-1,3,7C, (b) Xt-3,7C, and (c) Xt-1,3C adsorptions.

Caffeine (Xt-1,3,7C), theobromine (Xt-3,7C), and theophylline (Xt-1,3C) have been studied as passivators between HTL and $(FAPbI_3)_x(MAPbBr_3)_{1-x}$ PVK (where FA is formamidine, x is 0.92 in the precursor). While Xt-1,3C@PVK exhibited a PCE enhancement from 21.02% to 23.48% and long-term operational stability. PCEs of Xt-1,3,7C@PVK and Xt-3,7C@PVK are 22.32% and 20.24%, respectively. We made use of our methods and models above to partly explain their experimental

results. In Fig. S15, there are the configurations obtained by AIMD and geometry optimization of these three modified surfaces, and relevant data are in Table S5. As for adsorption energies, Xt-1,3C@PVK is stronger than Xt-1,3,7C@PVK. One more methyl group provides Xt-1,3,7C@PVK with a bigger steric hindrance so that the angle with the surface is larger than Xt-1,3C@PVK. Though the adsorption energy is strong for Xt-3,7C@PVK, similar to the conclusion of Wang et al, its adsorption sites (two Pb-O bonds and one -NH···I interaction) are too concentrated, and it also cannot lie flat on the surface. This may lead to an unstable surface, and therefore give a worse performance than the control device. The three adsorption sites of Xt-1,3C@PVK are arrayed triangularly, making it stably absorbs on the surface. The three's electronic states are similar without defect bands, resulting in sound PCEs.

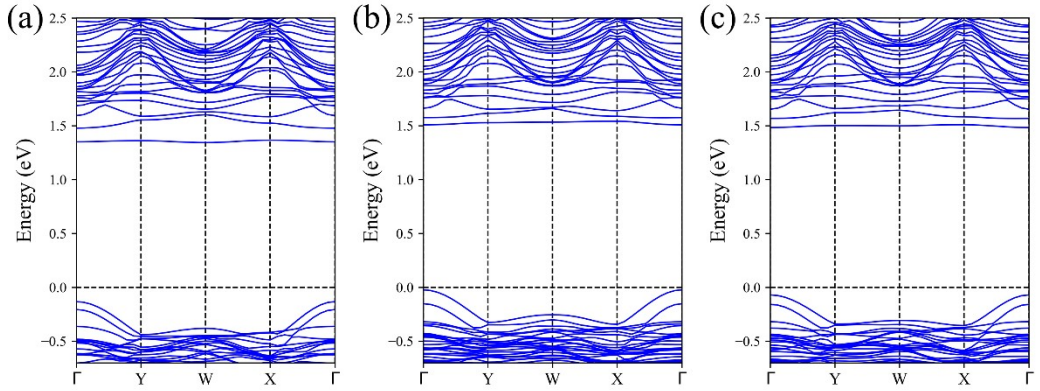

Fig. S16 Band structures of (a) TUA, (b) TUA-1,3C, and (c) TUA-1,7C adsorptions.

According to the study results of the LGs above, -C(=O)N and -C(=S)N functional groups exhibit strong adsorption with Pb sites. 7H-purine adsorption has multiple adsorption sites, giving the second strongest adsorption energy and small effective mass, without any midgap defect band, which can be an appropriate LG or FG. Xanthine and uric acid combined the two parts. Uric acid has been studied in the passivation of Sn-based PVK.[18] Due to the matching lattice constant, their two (or three) -C(=O)N functional groups can bind with two (or three) Pb sites. And the C=N-C functional group on 7H-purine can passivate the Pb ion, The -NH group on 7H-purine can also interact with the I ion. Moreover, we change the methyl groups and replace the O atoms with S atoms (Fig. S14) to design modifiers. Relevant data are in Table S5. Because the C-S bond is longer than C-O, the thio-substituted derivatives better match the $MAPbI_3$ lattice. The longer Pb-S bond also reduces the steric hindrance. The sulfur substitution molecules are all with better adsorption energies than the original ones. The molecules with 1,7-methyl substitution have better adsorption energies than the ones with 1,3-methyl substitution, due to their multi-site adsorption. UA-1,7C and TUA-1,7C have two -NH groups interacting with I sites, more than UA-1,3C and TUA-1,3C. However, for TUA and its methyl-substituted derivatives, a shallow defect band appears near the CBM, indicating that they may not be a good choice for modification (Fig. S16).

Table S5 Data for derivatives from xanthine and uric acid. *Linkage* represents the site linking to Pb ion, while the number represents the site number based on purine. n (H···I) represents the number of hydrogen bonds. m_{VB}^{*} represents the harmonic mean of m_{VB1}^{*}, and m_{VB2}^{*}. The effective mass unit is m_0 (the static mass of a free electron).

Notion of molecule	Linkage	Length (Å)	Angle (°)	E_{ads} (eV)	N_{tran} (e^-)	DM (a.u.)	WFS (eV)	n (H···I)	m_{VB1}^{*}	m_{VB2}^{*}	m_{VB}^{*}
Xt	2O, 9N	2.649, 2.703	~60	-1.216	0.060	0.122	-0.296	1	-0.229	-0.207	--0.217
Xt-1,3,7C	2,6O	2.689, 2.549	~30	-1.247	0.031	0.500	-0.487	0	-0.24	-0.195	-0.215
Xt-3,7C	2,6O	2.729, 2.571	~30	-1.393	0.026	0.509	-0.434	1	-0.224	-0.194	-0.208
Xt-1,3C	2,6O	2.721, 2.556	0~30	-1.315	0.017	0.416	-0.377	1	-0.230	-0.194	-0.210
TXt-1,3C	2,6S	3.025, 2.943	0~30	-1.520	0.188	0.244	-0.473	0	-0.245	-0.194	-0.217
UA	2,6,8O	2.654, 2.698, 2.894	~0	-1.474	-0.026	-0.094	-0.262	2	-0.208	-0.206	-0.207
UA-1,3C	6,8O	2.566, 2.569	0~30	-1.604	0.033	0.292	-0.393	1	-0.248	-0.197	-0.220
UA-1,7C	2,8O	2.693, 2.556	0~30	-1.865	-0.036	-0.296	-0.213	2	-0.208	-0.243	-0.224
TUA	2,6,8S	3.035, 3.130, 3.058	~0	-1.888	0.173	-0.153	-0.415	2	-0.223	-0.205	-0.213
TUA-1,3C	2,6,8S	3.113, 3.058, 3.039	~0	-1.865	0.197	0.084	-0.428	1	-0.239	-0.194	-0.214
TUA-1,7C	2,8S	2.993, 3.131, 2.949	0~30	-2.116	0.201	-0.093	-0.432	2	-0.245	-0.202	-0.221

Reference

1. Y. Wu, Y. Wang, J. Duan, X. Yang, J. Zhang, L. Liu and Q. Tang, *Electrochimica Acta*, 2020, **331**.
2. J.-W. Lee, S.-H. Bae, Y.-T. Hsieh, N. De Marco, M. Wang, P. Sun and Y. Yang, *Chem*, 2017, **3**, 290-302.
3. L. Gao, S. Huang, L. Chen, X. Li, B. Ding, S. Huang and G. Yang, *Solar RRL*, 2018, **2**.
4. N. K. Noel, A. Abate, S. D. Stranks, E. S. Parrott, V. M. Burlakov, A. Goriely and H. J. Snaith, *ACS nano*, 2014, **8**, 9815-9821.
5. X. Liu, J. Wu, Q. Guo, Y. Yang, H. Luo, Q. Liu, X. Wang, X. He, M. Huang and Z. Lan, *Journal of Materials Chemistry A*, 2019, **7**, 11764-11770.
6. Y. Zhang, G. Grancini, Z. Fei, E. Shirzadi, X. Liu, E. Oveisi, F. F. Tirani, R. Scopelliti, Y. Feng, M. K. Nazeeruddin and P. J. Dyson, *Nano Energy*, 2019, **58**, 105-111.
7. H. Zhang, H. Chen, C. C. Stoumpos, J. Ren, Q. Hou, X. Li, J. Li, H. He, H. Lin, J. Wang, F. Hao and M. G. Kanatzidis, *ACS Appl Mater Interfaces*, 2018, **10**, 42436-42443.
8. M.-S. Lee, S. Sarwar, S. Park, U. Asmat, D. T. Thuy, C.-h. Han, S. Ahn, I. Jeong and S. Hong, *Sustainable Energy & Fuels*, 2020, **4**, 3318-3325.
9. F. Wang, W. Geng, Y. Zhou, H.-H. Fang, C.-J. Tong, M. A. Loi, L.-M. Liu and N. Zhao, *Advanced Materials*, 2016, **28**, 9986-9992.
10. S. Zhao, J. Xie, G. Cheng, Y. Xiang, H. Zhu, W. Guo, H. Wang, M. Qin, X. Lu, J. Qu, J. Wang, J. Xu and K. Yan, *Small*, 2018, **14**, e1803350.
11. G. Li, J. Wu, J. Song, C. Meng, Z. Song, X. Wang, X. Liu, Y. Yang, D. Wang and Z. Lan, *Journal of Power Sources*, 2021, **481**.
12. J. Xue, R. Wang and Y. Yang, *Nature Reviews Materials*, 2020, **5**, 809-827.
13. J. Haruyama, K. Sodeyama, L. Han and Y. Tateyama, *J Phys Chem Lett*, 2014, **5**, 2903-2909.
14. W. Ming, S. Chen and M.-H. Du, *Journal of Materials Chemistry A*, 2016, **4**, 16975-16981.
15. W.-J. Yin, T. Shi and Y. Yan, *Applied Physics Letters*, 2014, **104**.
16. Y. Zhou and A. Gray-Weale, *Physical Chemistry Chemical Physics*, 2016, **18**, 4476-4486.
17. R. Wang, J. Xue, K. L. Wang, Z. K. Wang, Y. Luo, D. Fenning, G. Xu, S. Nuryyeva, T. Huang, Y. Zhao, J. L. Yang, J. Zhu, M. Wang, S. Tan, I. Yavuz, K. N. Houk and Y. Yang, *Science*, 2019, **366**, 1509-1513.
18. H. Mohammadian-Sarcheshmeh, M. Mazloum-Ardakani, M. Rameez, S. Shahbazi and E. W.-G. Diau, *Journal of Alloys and Compounds*, 2020, **846**.

Configurations and Band structures for All Calculated Modified Surfaces

CO@PVK:

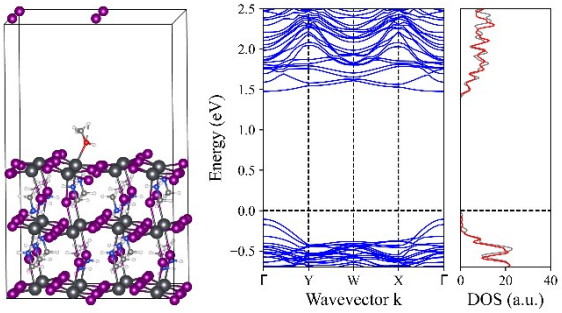

COC@PVK:

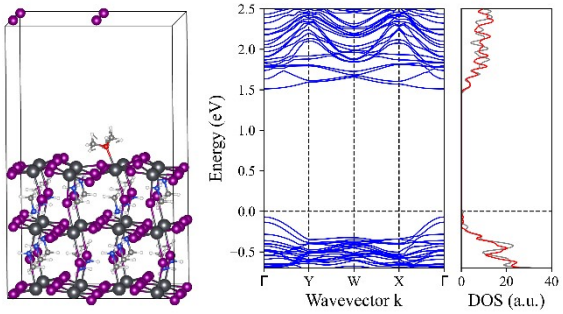

CS@PVK:

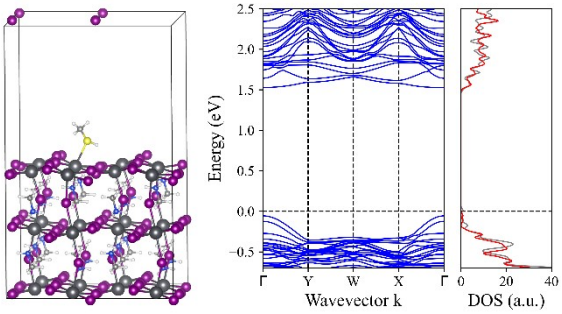

CSC@PVK:

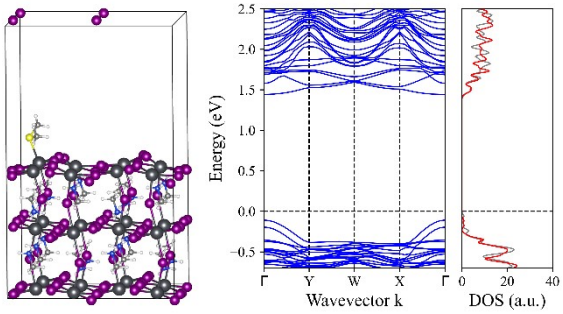

CN@PVK:

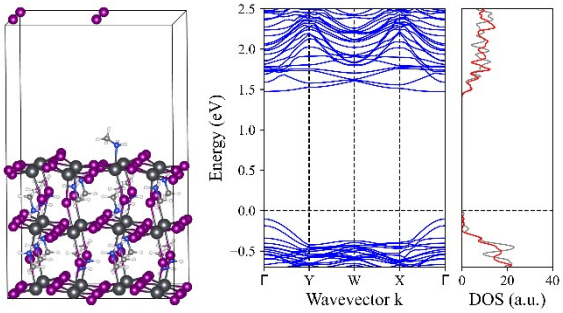

CN(C)C@PVK:

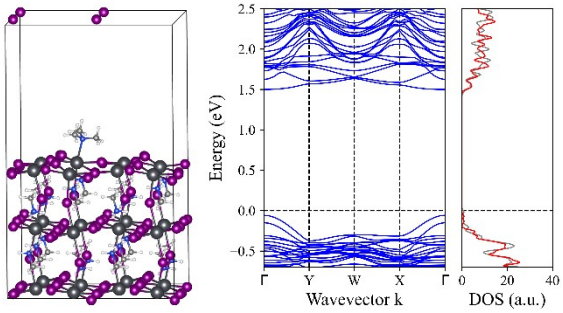

CN=NC@PVK:

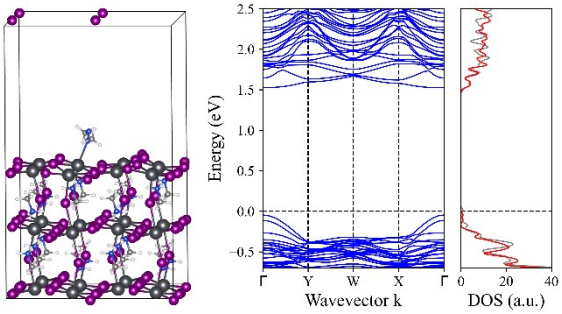

CC≡N@PVK:

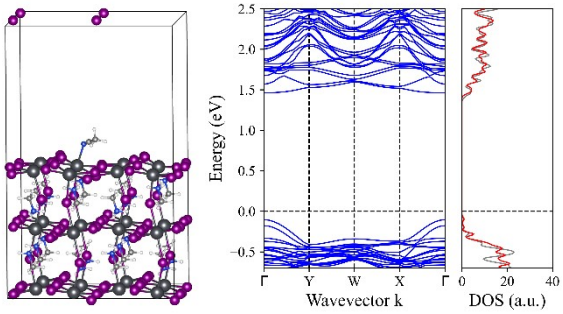

CC(=O)C@PVK:

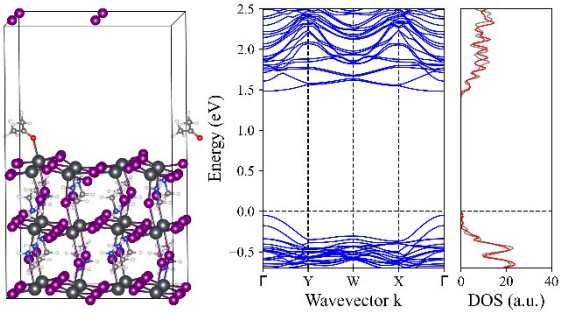

CC(=O)N@PVK:

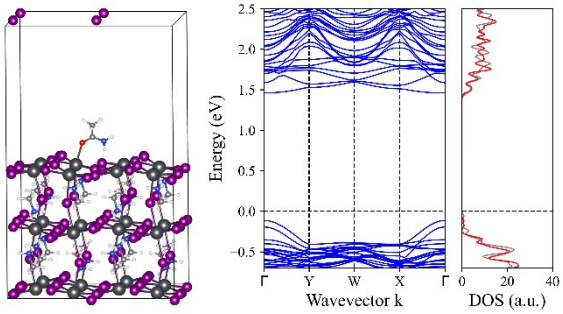

NC(=O)N@PVK:

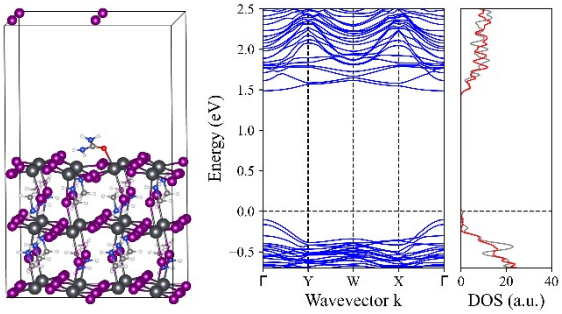

CC(=S)C@PVK:

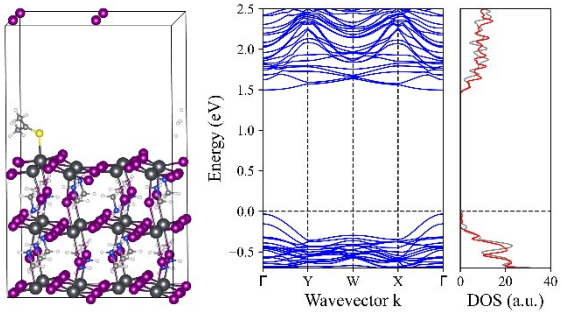

CC(=S)N@PVK:

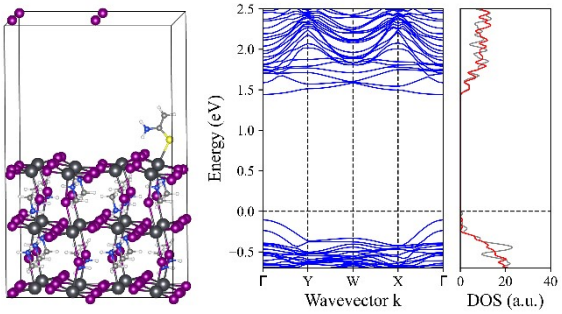

NC(=S)N@PVK:

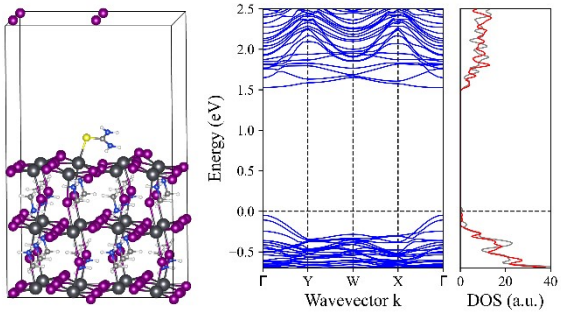

CC(=O)O@PVK:

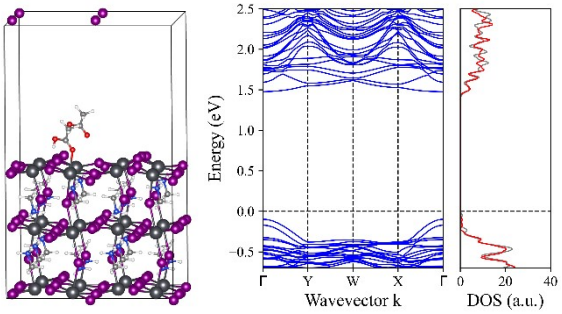

CC(=O)OC@PVK:

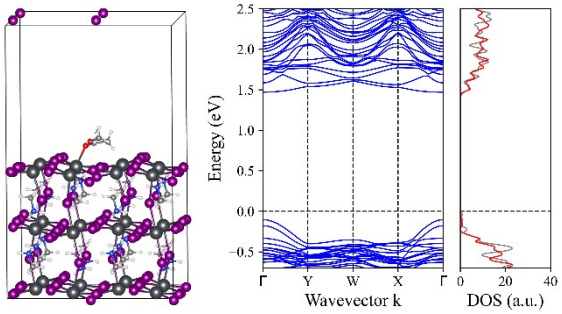

CC(=O)SC@PVK:

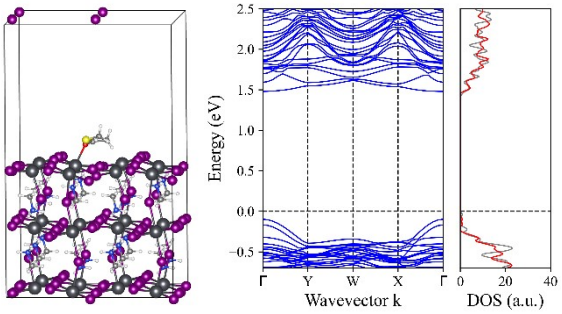

CS(=O)(=O)C@PVK:

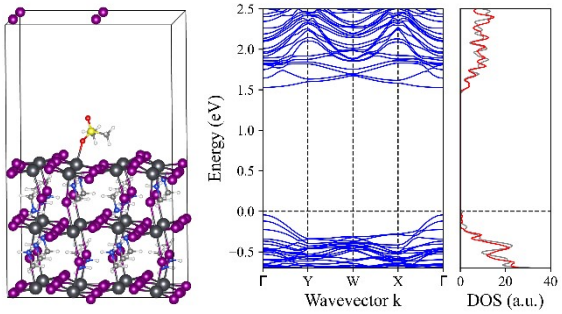

CS(=O)(=O)N@PVK:

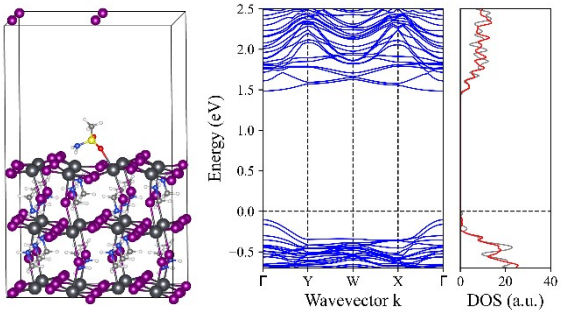

R5-O@PVK:

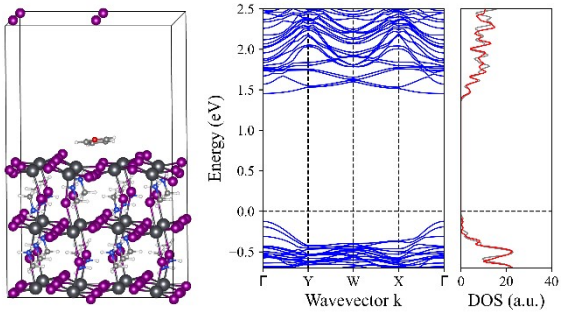

R5-S@PVK:

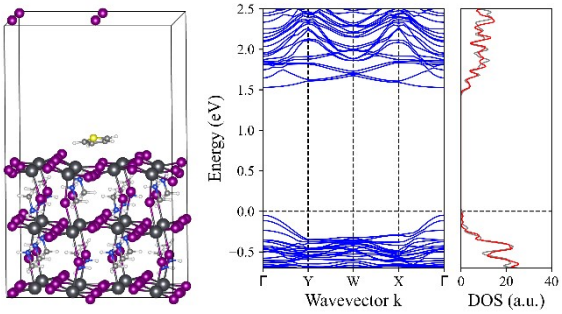

R5-N@PVK:

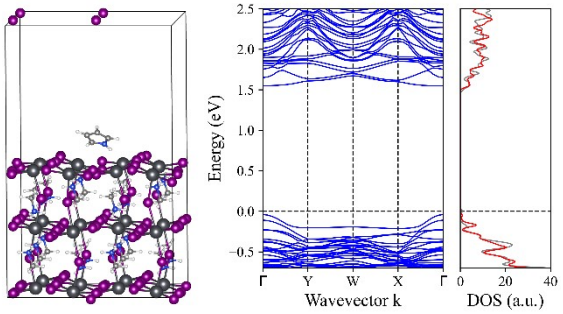

R5-2N@PVK:

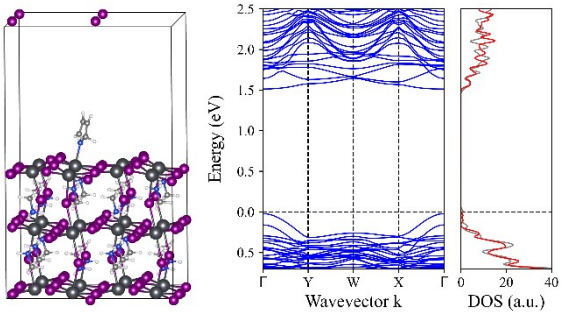

R5-3N@PVK:

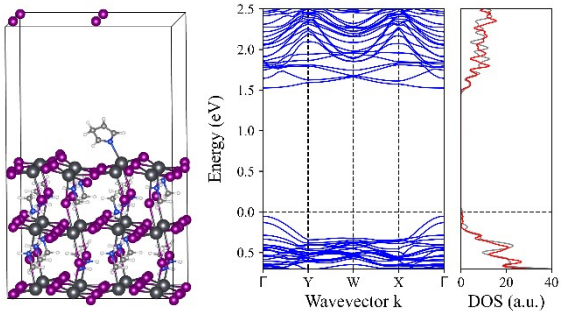

R5-1,2N@PVK:

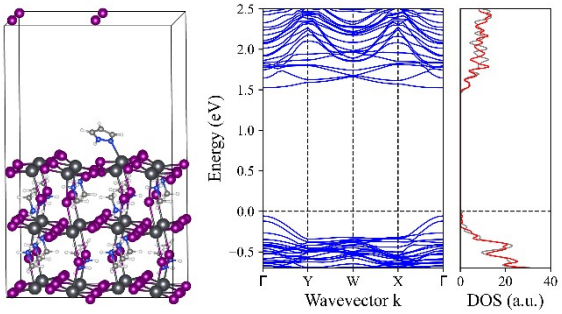

R5-1,3N@PVK:

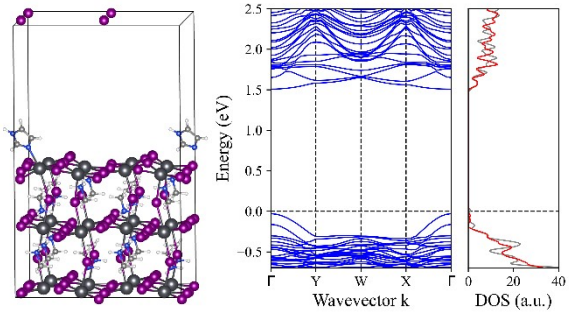

R5-1,2,4N@PVK:

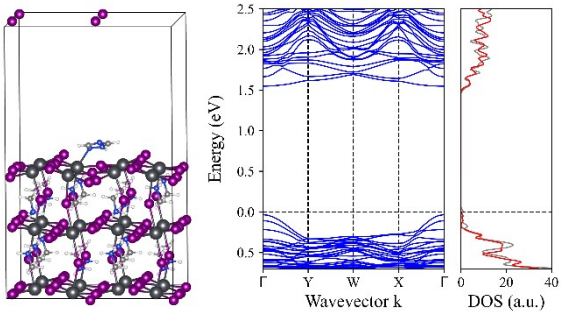

R5-O-3N@PVK:

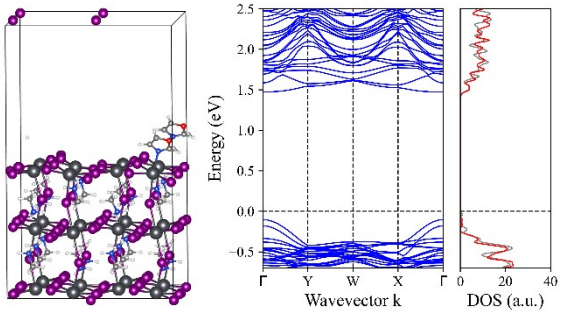

R5-S-3N@PVK:

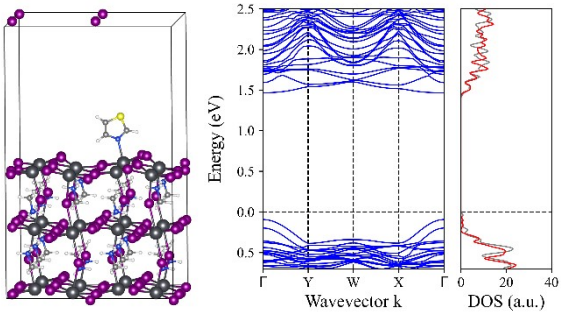

R6-N

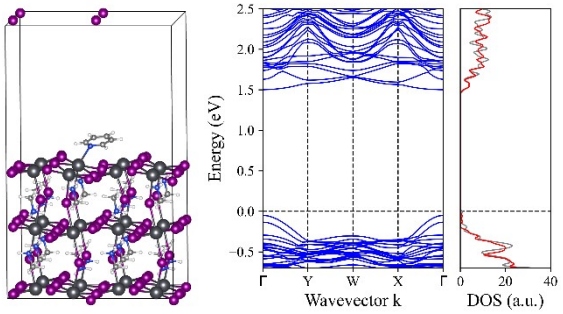

R6-1,2N@PVK:

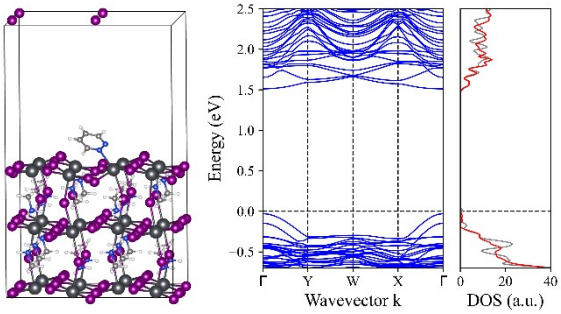

R6-1,3N@PVK:

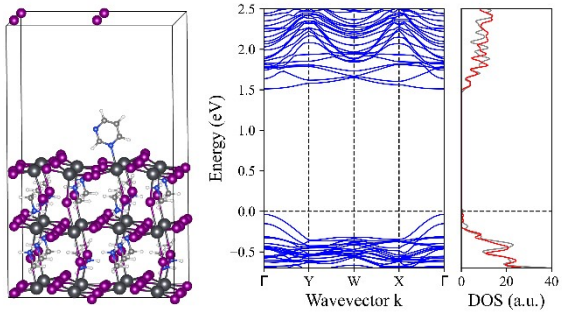

R6-1,4N@PVK:

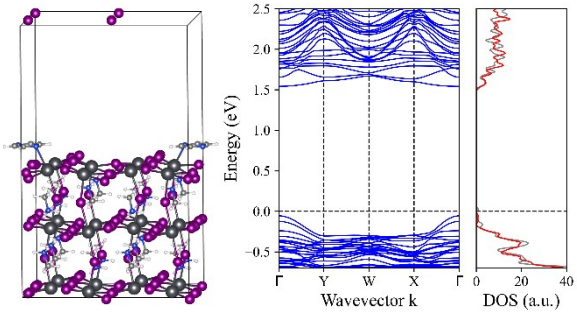

R6-1,2,4N@PVK:

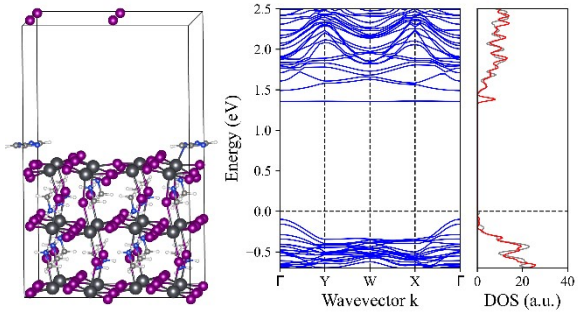

R6-1,3,5N@PVK:

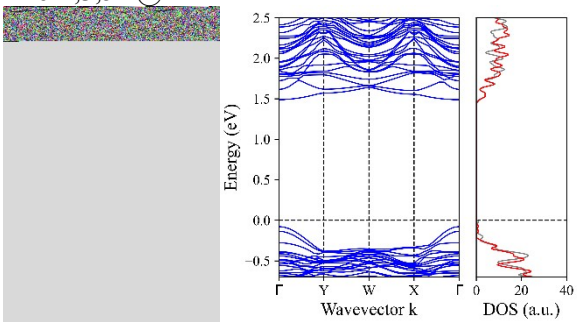

R6-O-4H@PVK:

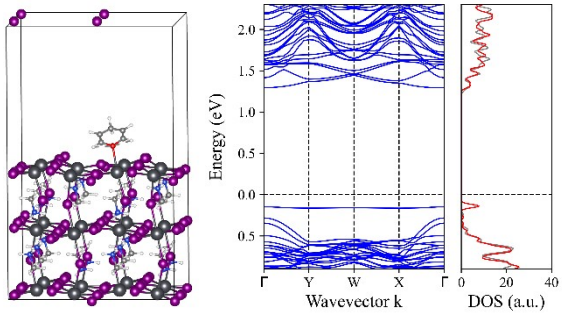

R6-1,4O@PVK:

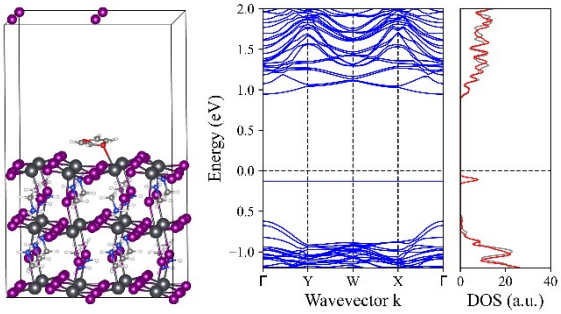

Ph@PVK:

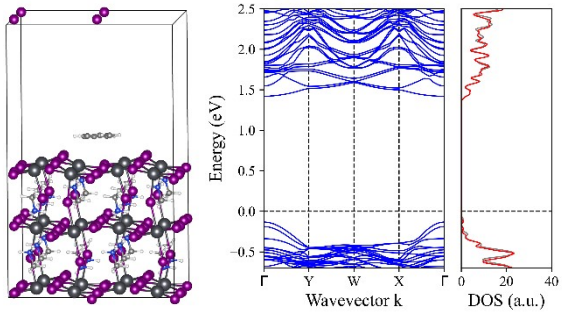

Ph-F@PVK:

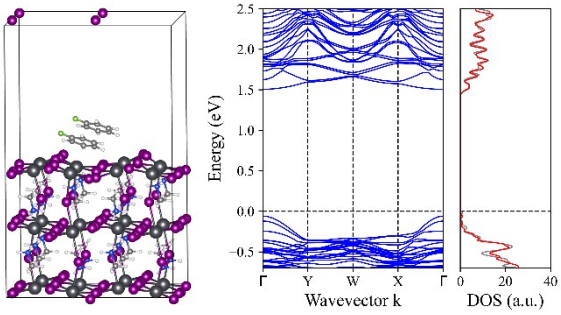

Ph-C@PVK:

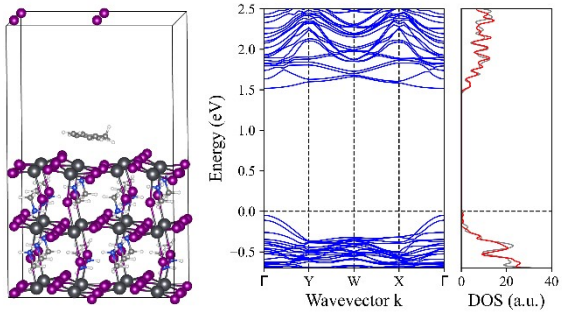

Ph-O@PVK:

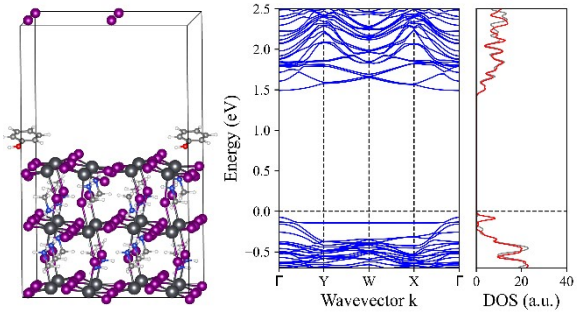

Ph-S@PVK:

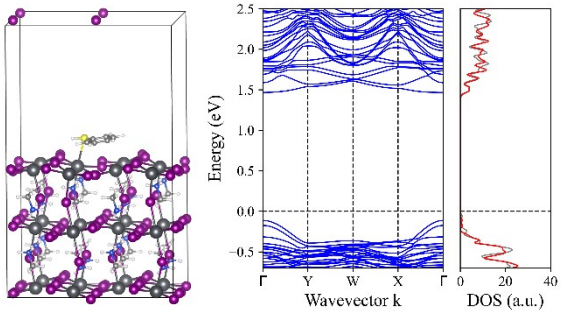

Ph-N@PVK:

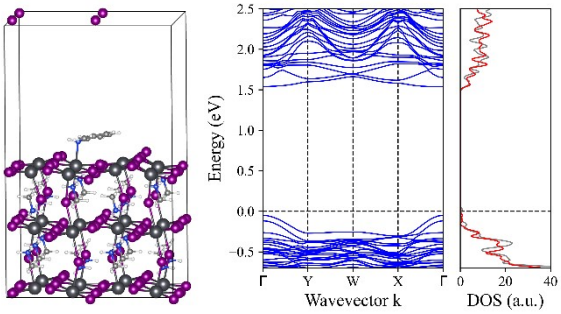

PH-N-4F@PVK:

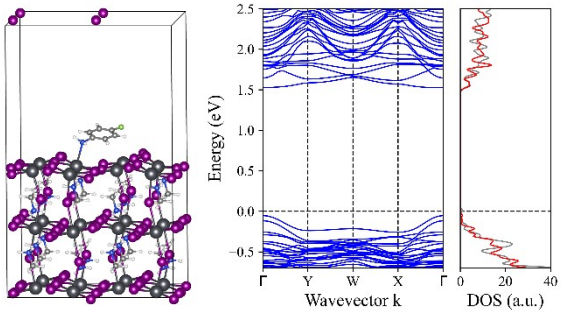

PH-N-2,4,6F@PVK:

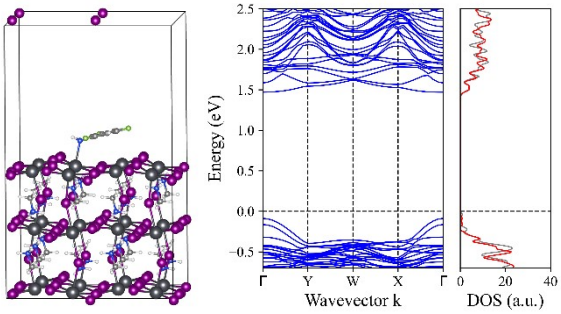

PH-N-2,3,4,5,6F@PVK:

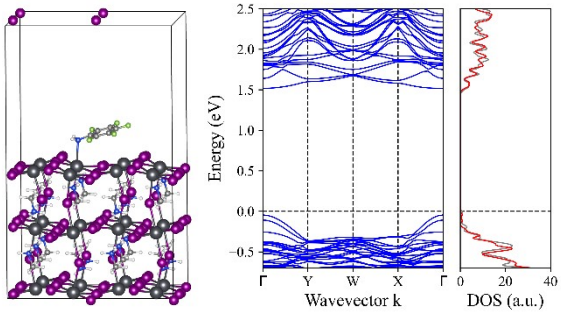

naphthalene@PVK:

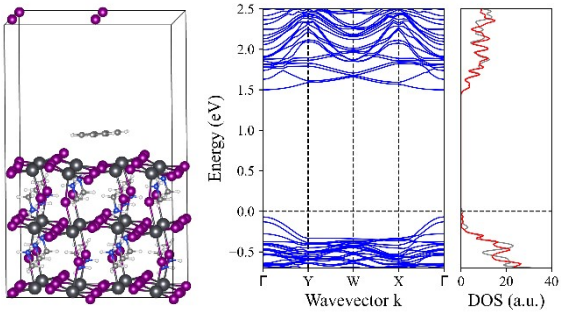

1H-indole@PVK:

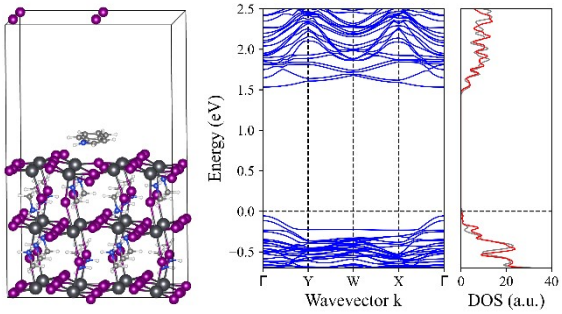

quinoline@PVK:

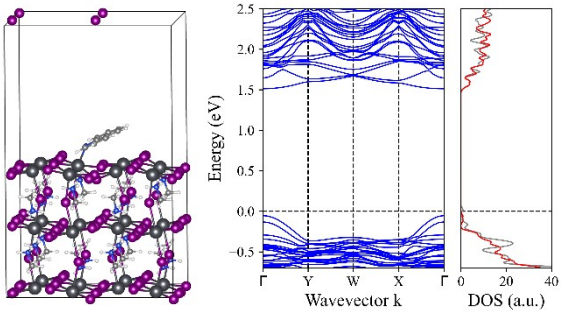

7H-purine@PVK:

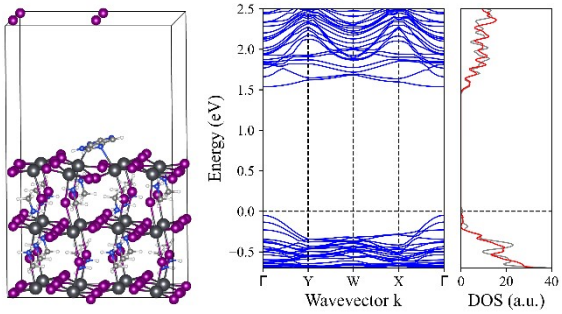

3-phenylpyrrole@PVK:

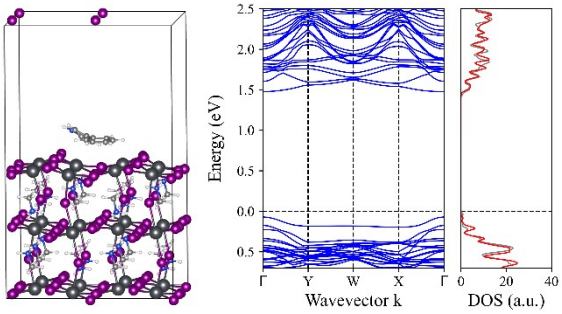

4-phenylpyridine@PVK:

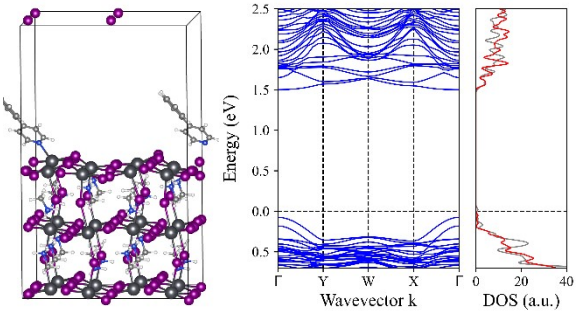

2-thiophenamine@PVK:

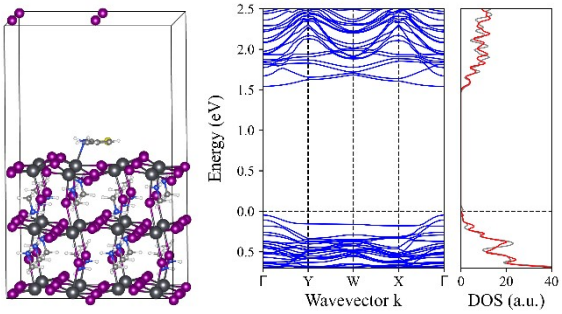

3-thiophenamine@PVK:

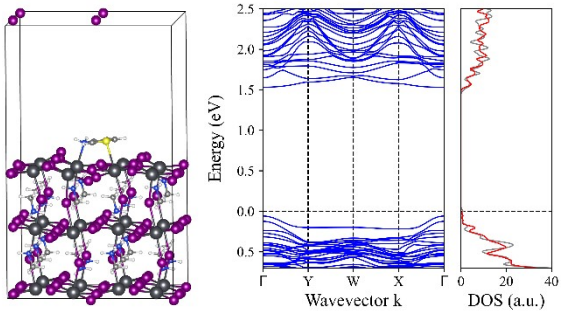

Xt@PVK:

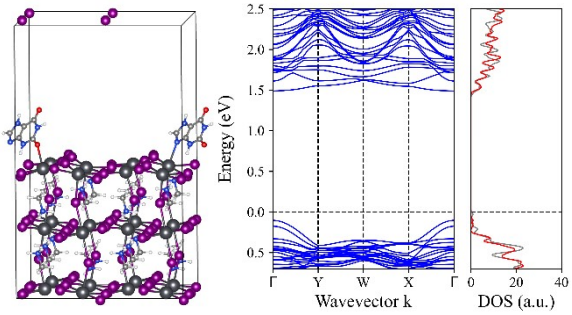

Xt-1,3,7C@PVK:

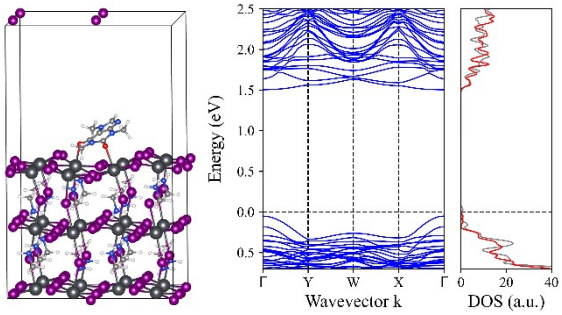

Xt-3,7C@PVK:

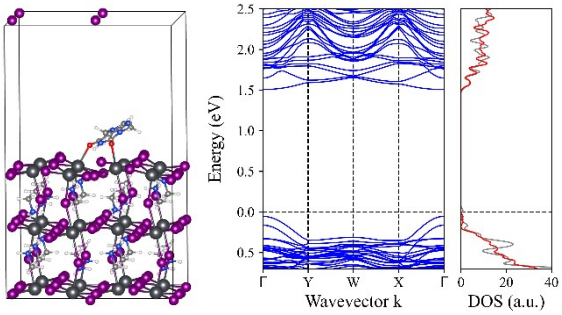

Xt-1,3C@PVK:

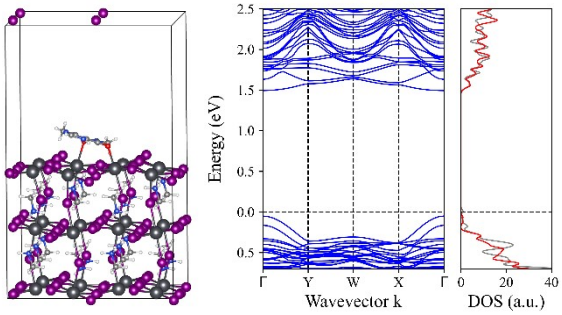

TXt-1,3C@PVK:

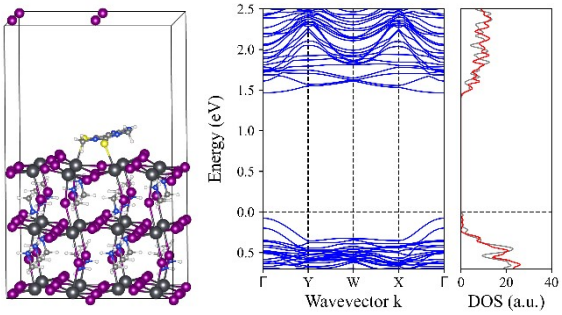

UA@PVK:

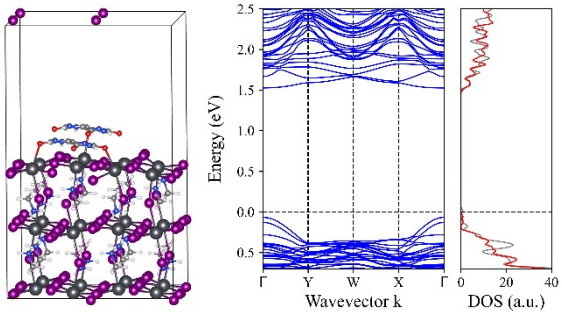

UA-1,3C@PVK:

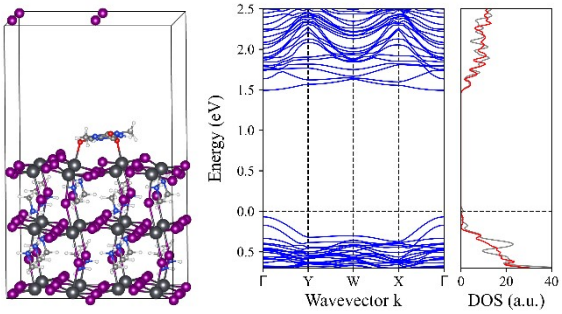

UA-1,7C@PVK:

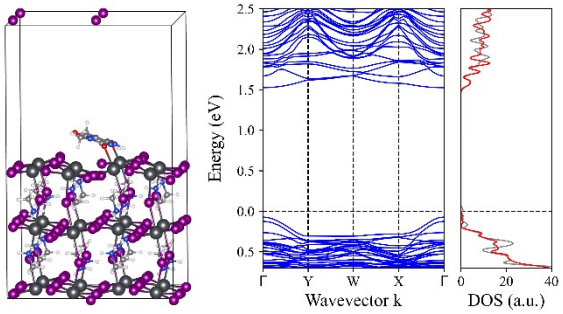

TUA@PVK:

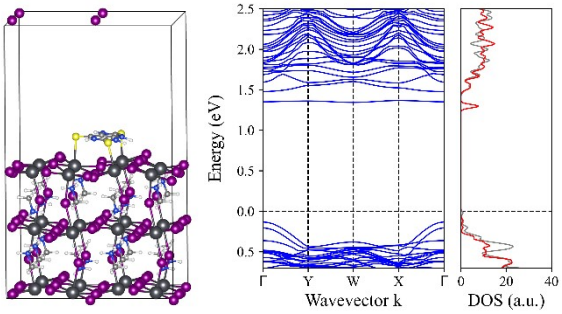

TUA-1,3C@PVK:

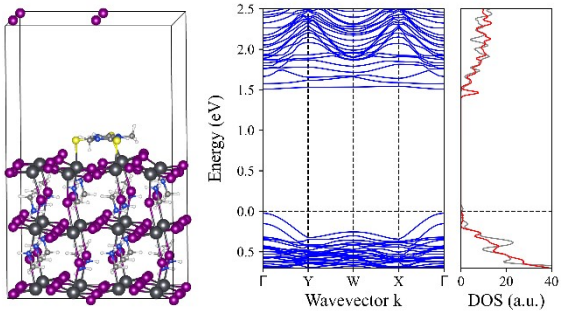

TUA-1,7C@PVK: